Simulation and Performance Analysis of Cellular Digital Packet Data

by

J. Scott Elson

Thesis submitted to the faculty of the
Virginia Polytechnic Institute and State University
in partial fulfillment of the requirements of

MASTER OF SCIENCE

IN

ELECTRICAL ENGINEERING

APPROVED:

Dr. Jeffrey H. Reed, Chairman

Dr. Brian D. Woerner

Dr. Ira Jacobs

February, 1996

Blacksburg, Virginia

Key Words

Cellular Digital Packet Data (CDPD), Gaussian Minimum Shift Keying (GMSK), Reed-Solomon Codes, Frequency Discriminator, Differential Detection

Simulation and Performance Analysis of Cellular Digital Packet Data

by

J. Scott Elson

Committee Chairman: Dr. Jeffrey H. Reed

Electrical Engineering

(ABSTRACT)

As the wireless telecommunications industry becomes more widely accepted, the need for mobile data communication has followed the rise in mobile voice communication. Cellular Digital Packet Data (CDPD) offers an unobtrusive data service that overlays the existing Advanced Mobile Phone Service (AMPS) in a cost effective manner that will be attractive to most service providers. Using idle time between voice traffic, CDPD uses Gaussian Minimum Shift Keying (GMSK) to send bursts of Reed-Solomon encoded information while channel hopping to avoid interfering with voice transmissions.

This thesis assesses the performance of CDPD for different channel environments through simulation. Specifically, Gaussian noise, Rayleigh fading, co-channel interference models are incorporated to identify the performance of the system.

Key Words

Cellular Digital Packet Data (CDPD), Gaussian Minimum Shift Keying (GMSK), Reed-Solomon Codes, Frequency Discriminator, Differential Detection

ACKNOWLEDGEMENTS

I wish to express my sincere thanks to Dr. Jeff Reed for acting as my advisor and for his patience, motivation, encouragement, and most of all guidance which have been invaluable towards the completion of this work. I would also like to thank Dr. Brian Woerner and Dr. Ira Jacobs for serving on my committee as well.

A special thanks goes to Grayson Electronics for providing the resources to make this research possible.

Thanks as well to Jay Jacobsmeyer of Pericle Communications Company and Steve Gardner at PCSI for their feedback along the way.

I would also like to thank Dr. Joe Liberti for his helpful advice and his many insightful conversations which proved invaluable to the completion of this thesis. I also thank Prabhakar Koushik for his expertise as system administrator. I value their assistance as well as their friendship.

I am also grateful to everyone at MPRG for making the many hours I have spent there a pleasurable experience and one I am thankful to have had.

Lastly, I would like to thank my family who has always given me support and encouragement in all aspects of my life and who's love and presence I feel at all times.

Table Of Contents

List Of Figures

List Of Tables

Chapter 1

Introduction

To this day, little technical research has focused on the performance of Cellular Digital Packet Data (CDPD). This is partially due to the CDPD's relatively young age and scarce deployment. As CDPD roll out grows this information becomes increasingly important but tends to remain confidential to the cellular providers. This work is intended to make performance analysis of CDPD available as public information.

1.1 Cellular Background

Telecommunications is rapidly moving towards an era of increasing mobility with the goal of freeing users of their wired environment. With advancements in radio engineering and increased radio frequency (RF) spectrum availability, mobile communications is moving beyond its original application for voice and is becoming a popular medium to send and receive data and video as well.

Currently, the widest implementation of cellular technology in the United States is the Advanced Mobile Phone Service (AMPS). This system is made up of mobile terminals, cell sites, and Mobile Telephone Switching Offices (MTSOs). A mobile terminal can be any portable cellular device that can send and receive voice signals. Cell sites provide the interface between the mobile terminals and the MTSO. The MTSO coordinates a number of cell sites and mobile terminals, acting as a cellular "switch" for calls and providing a connection to land lines, while also keeping track of billing information.

The Federal Communications Commission (FCC) has allocated 50 megahertz (MHz) of the frequency spectrum to be used for cellular communications. This 50 MHz is

broken up into two 25 MHz sections. The frequencies for forward communications (cell to mobile) are located between 869 MHz to 894 MHz, while the frequencies for reverse communications (mobile to cell) are located between 824 MHz to 849 MHz. The 20 MHz gap in the cellular band helps minimize interference between forward and reverse communications. For cellular voice communications, one forward and one reverse connection is required for each call. Each connection uses a pair of 30 kilohertz (KHz) channels, giving 832 channel pairs available in the cellular domain. These channel pairs are halved into an A and B side which must be managed by separate telecommunications providers. Other 30 KHz channels, called control channels, exist within the 800 MHz band and are used to setup calls between mobiles and cell sites.

When powered on, the mobile will monitor the cellular frequency spectrum for the strongest available control channel. When a call begins, the mobile locks on to this channel and starts exchanging data with the nearest cell site. This data includes the numbers of both parties and electronic serial numbers. After the mobile is validated as an credible user, the cell instructs the mobile to change frequency to a particular voice channel for communication, connecting both parties. During a call, the mobile may move outside the cell's coverage area and will need to be transferred to another cell site. When this happens, the MTSO is responsible for maintaining the connection by initiating a hand-off to the new cell. The MTSO determines which surrounding cell site would provide the strongest available signal for the mobile and sets up the new communications between the two.

These procedures provide the basis for the operation of the AMPS cellular system and the infrastructure for wireless voice communications. What follows is a discussion of the extension of these procedures to include data services as well, specifically focusing on Cellular Digital Packet Data or CDPD.

1.2 Networking and Cellular Data

A network is a group of computing devices that can be connected in order to share information. Each device is assigned a unique number called a network address (much like a telephone number) to make this sharing possible. Using an addressing technique, computers can directly communicate with each other over the network. Figure 1-2 below shows the concept of a generic network where computers A, B, and C can communicate with each other.

Every network has a defined set of protocols which establishes the rules and formats for communication within that network. Any applications or products developed within that network will then be compatible with each other. For example, if a word processing application is created using the protocols defined in Figure 1-1's network, then computer A and computer B will be able to use it whether it is running off a local disk or a remote host (computer C). To solve the problem of network incompatibility between different types of computing devices, translation or conversion equipment has to be used. Combining these ideas with the concept of wireless communication gives rise to the notion of a cellular network.

Sending data over cellular was envisioned by early pioneers who realized its promise, building equipment that allowed computers and faxes to transmit data over cellular using standard voice channels. These systems were circuit-switched, meaning they took control of an entire voice channel for an entire data transmission. Using circuit-switched technology, data can be sent by attaching a wireless modem to a computing device such as a laptop computer. The modem translates the digital data into an analog signal and transmits the data over the cellular network to another modem capable of translating the data back to digital form. Connections with cell sites are established in the same manner as with voice calls, and once a channel is locked by a user, data is transmitted instead of

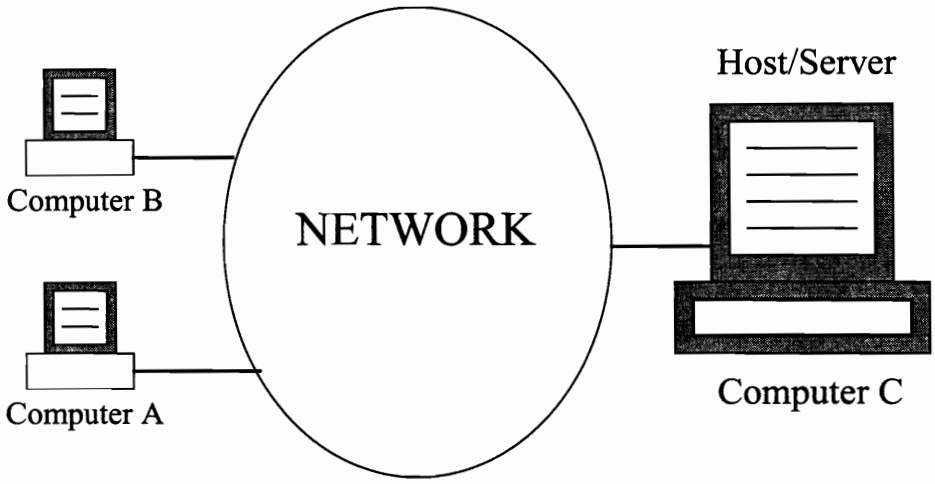

Figure 1-1: Generic Network

voice.

Circuit-switching can be used to transmit any type of data, but is best suited for large transfers such as faxes. Short data transfers using circuit-switching are not as efficient because of the large amount of overhead involved in the setup and tear down while establishing a cellular connection. For these types of transactions, packet-switched techniques such as CDPD are more suitable.

1.3 CDPD Network Entities

The implementation of CDPD in the current cellular infrastructure requires the installation of new equipment at cell sites and a means of networking the data. Much of this equipment serves the same purpose as its AMPS counterpart, only it is used for digital data. There are two basic classes of CDPD network entities called End Systems (ESs) and Intermediate Systems (ISs). ESs are the CDPD network hosts and ISs are the network routers.

1.3.1 End Systems

End systems communicate with each other over the CDPD network like a telephone, except it is used to send and receive digital data. There are two types of end systems in the CDPD network - Mobile End Systems (M-ESs) and Fixed End Systems (F-ESs).

M-ESs are portable wireless computing devices such as Personal Digital Assistants that roam from site to site and communicate with the network using a CDPD modem. M-ESs are smarter than cellular phones in that the decision to initiate a transfer, or hand-off, from one cell to another is made by the M-ES itself rather than the MTSO. The M-ES monitors the received signal strength indicator (RSSI) of the cellular channels and if the RSSI drops below a predetermined level, the M-ES will transfer to a new channel or cell. Communication between the M-ESs and the CDPD network takes place over an Airlink Interface. As with voice communication, it requires a channel pair. The Airlink Interface encrypts data sent over these channels for non-broadcast/multicast applications to prevent eavesdropping while also employing error correction.

F-ESs are servers or tethered host systems which are directly wired to the CDPD network. F-ES configuration and applications do not have to be modified for the CDPD network and F-ESs can communicate with M-ESs in the same way they do with other F-ESs. Although they are located in external networks, F-ESs can still communicate with the CDPD network through an external interface. F-ESs communicate using an External Interface which may include existing networks such as Internet, OSInet or other external networks having compatibility with the CDPD network. CDPD distinguishes between M-ESs and F-ESs for mobility management.

1.3.2 Intermediate Systems

New internal entities need to be added to modify the existing cellular infrastructure in order to incorporate CDPD technology. These are the Mobile Data Intermediate System (MD-IS), the Mobile Data Base Station (MDBS), and the Intermediate Systems (IS). These entities are integrated with and overlay their cellular voice equivalents.

The MD-IS is a stationary network component which has similar responsibilities as the MTSO mentioned earlier. As the MTSO is responsible for tracking a cellular phone's location and the routing of calls, the MD-IS is responsible for keeping track of the M-ESs location and routing data packets to and from the CDPD network and the M-ES appropriately. MD-ISs are responsible for making sure a M-ES is valid to log on the network while also storing information such as the M-ES's last known location, traffic statistics and billing information. MD-ISs are the only intermediate systems in the CDPD network that have any knowledge of mobility for M-ESs in the system and operate a specific Mobile Network Location Protocol (MNLP) to exchange location information between themselves. This exchange of information allows the MD-ISs to operate the packet forwarding service which allows an M-ES to travel anywhere in the cellular domain without losing connectivity.

The MDBS is a stationary network component that is primarily responsible for relaying data between M-ESs and the MD-IS and the management of the RF channels. The MDBS has a scanning receiver that observes all AMPS channels to detect the presence of voice traffic based on signal strength. If two channels (one transmit, one receive) are idle, the MDBS will establish an air link between itself and an M-ES that wants the channels for transmission. The MDBS is fast enough to detect when an analog voice signal is coming up on an established air link RF channel. It takes approximately 40 milliseconds (msec) for a channel to ramp up before voice is transmitted, which is sufficient of time for the MDBS to instruct the M-ES to hop to a new channel for continued communi-

cation, i.e., frequency hopping. The MDBS also aids the M-ES in making a cell transfer by assisting in the location of a new channel. It keeps track of all adjacent cell channels that are potentially usable for CDPD and broadcasts the list to the surrounding M-ESs so quick decisions can be made when necessary. In this way CDPD becomes transparent to the AMPS network in which it runs parallel.

All of the serving areas of the network are interconnected by a number of ISs. The IS equipment and the physical interconnections associated with each IS create the CDPD network backbone. ISs are routers that are CDPD compatible, having the primary responsibility of relaying data packets between MD-IS and other ISs throughout the system. Multiple ISs are configured so that there is more than one potential path between any two ISs. Since ISs are unaware of mobility, off-the-shelf routers that support Internet and OSI Connectionless Network Services (CLNSs) can be used throughout the backbone to interconnect the serving domains of other cellular carriers and external land-based networks. Figure 1-2 shows an overview of the CDPD network.

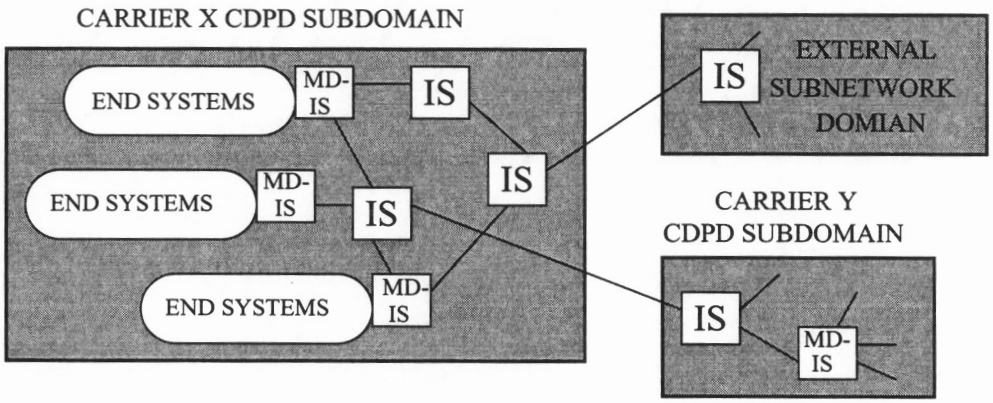

Figure 1-2: CDPD Network Architecture

ISs use an Inter-Service Provider Network Interface to allow different CDPD carriers to communicate and exchange information with each other. This means that CDPD

subscribers in Atlanta can communicate with CDPD subscribers in Seattle regardless of who is providing the local service. This interface supports CDPD network services across all geographic areas where CDPD is available including M-ES authentication, network management, and remote activation.

1.4 CDPD Specifics

1.4.1 CDPD Background

The first company to develop a packet-switched data system to be used over cellular was Cellular Data, Inc. (CDI), Palo Alto, CA [Merrill94], but their technology was obsolete even before it hit the market. In 1992, CDPD was recognized as a business solution for transmitting data over cellular and a need for standardization was foreseen because implementing CDPD technology could be done in a number of ways. For this very reason, the leaders of the cellular industry formed a CDPD consortium which included the following companies [CDPDW95]:

- Ameritech Mobile Communications
- Bell Atlantic Mobile Systems
- Contel Cellular
- GTE Mobile Communications
- McCaw Cellular Communications, Inc.
- NYNEX Mobile Communications, Inc.
- Pactel Cellular
- Southwestern Bell Mobile Systems

The new standard that superseded CDI was CDPD, a new system that is designed to transmit data using idle times between voice calls on the AMPS cellular infrastructure using channel (frequency) hopping. Unlike CDI, it was royalty free and available to developers

at no charge [Gall94]. *Cellular Digital Packet Data System Specification Release 1.0* was released by the CDPD consortium in July of 1993 and details the guidelines that were agreed upon. Since then, Release 1.1 has been published in January of 1995 incorporating a number of changes and refinements from the previous version.

The current AMPS cellular infrastructure is extensive with nationwide coverage, nevertheless is was designed specifically to transmit analog voice signals. The beauty of CDPD is that it provides a seamless national digital data overlay using the existing cellular network. It also efficiently uses frequencies that are otherwise idle. If CDPD can send a data burst during gaps in voice transmissions, it is effectively increasing the capacity of the system. However, CDPD can also use dedicated channels to transmit data if needed.

CDPD's packet switched nature allows users to be charged for the amount of data actually sent, not by the minute like regular call. CDPD is cost effective since equipment needs only be added to the existing cell sites. The cost of upgrading a cell site to CDPD is low relative to building an entire new site. Carriers only have to add a new base station at each cell site and packet switch at the MTSO.

ARDIS and RAM, two other mobile packet switched data networks, will see CDPD as a threat. ARDIS, the first nationwide packet data network, is a partnership of Motorola and IBM. Originally developed for its own engineers and field service personnel, ARDIS is now commercially available and has more than 30,000 users [Merrill]. It offers services ranging from RadioMail, its version of e-mail, to customized wireless solutions to companies with a large mobile workforce [ARDIS95].

RAM, a partnership of RAM Mobile Data and BellSouth, uses Mobitex®, the international standard for two-way wireless data communications currently operational in 17 countries worldwide, as its core technology. It claims to offer 100% on-street, in-vehicle and in-building U.S coverage with more than 1000 base stations today and 500 more base stations scheduled to be deployed within the next five years [RAM95]. These packet switched systems contend they can compete with CDPD, but with over 16,000 AMPS

sites in North America and growing, CDPD can almost guarantee universal coverage to subscribers, an advantage the other wide area networks can't.

1.4.2 Data Transformation and Transmission

The input to the CDPD network is digital data. At the network layer, this data is divided into packets called Network Protocol Data Units (NPDUs). Each NPDU is 2048 bytes in length and includes the user data along with an added header. The header contains important information including source and destination addresses. If any of the packets are received out of order, the receiving device can reassemble them in the original sequence. Before being sent over the airlink, the NPDUs must go through a transformation process that results in a stream of bits which are transmitted one at a time.

The following steps, shown in Figure 1-3 [CDPDS95], are undertaken to transform the NPDU for transmission:

- The packet header is compressed (optional)
- The packet is compressed (optional)
- The packet is segmented and each segment is provided with a segment header. Each segment may hold up to 128 bytes of user data.
- Each point-to-point segment (i.e. non broadcast/multicast) is encrypted for security over the airlink
- Each segment is encapsulated within a frame with a frame header. Each frame may contain up to 130 bytes of user data.
- The sequence of frames are transformed into an information bit stream by the insertion of frame flags to delimit frames from each other.
- The information bit stream is blocked into consecutive sets of bits and the blocks are subjected to Reed-Solomon forward error correction (detailed in Chapter 2). Each block has a fixed size which holds 282

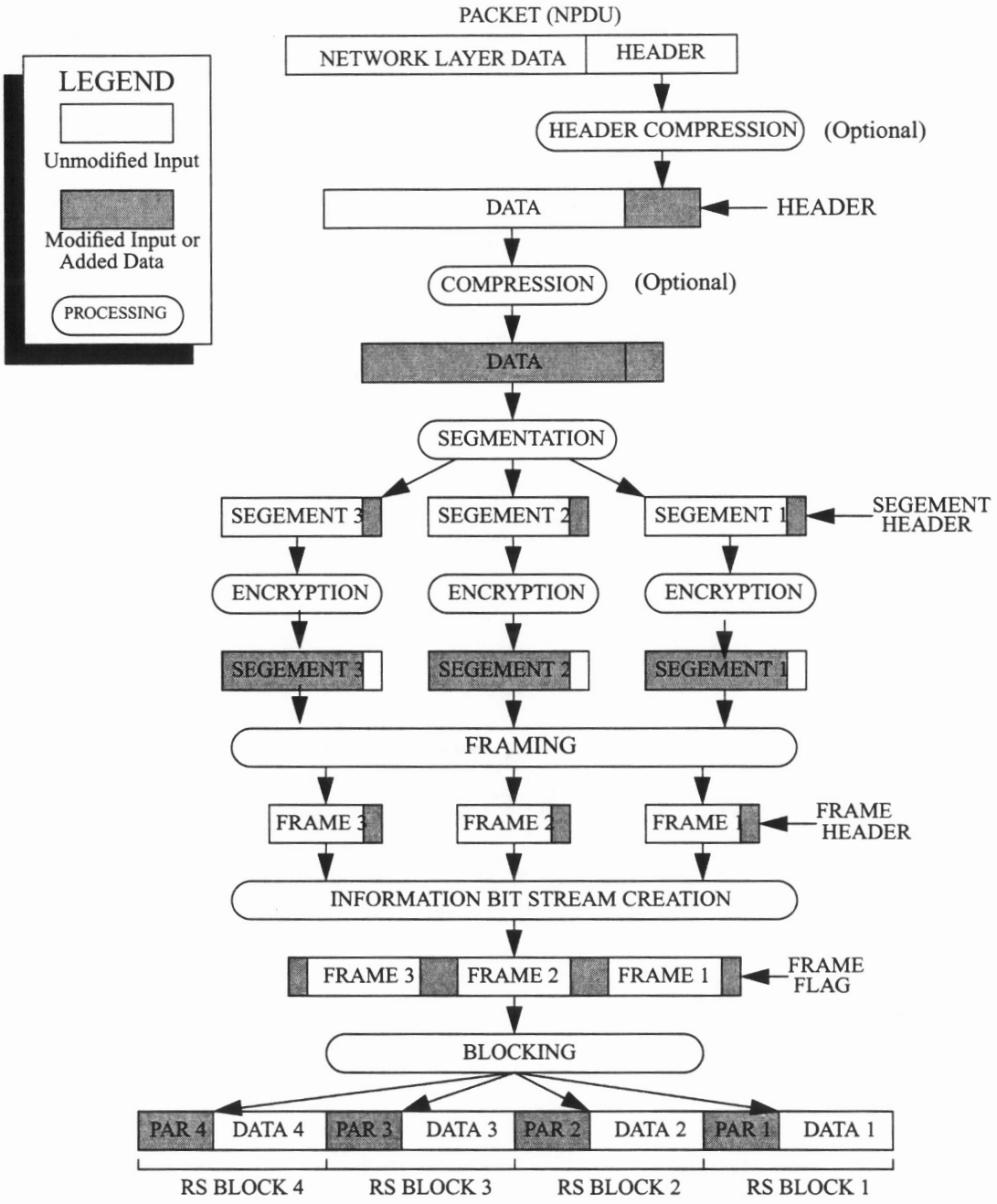

Figure 1-3: Data Packet Transformation

bits of data.

- Each block is transmitted as a sequence of bits over the airlink.

Upon reception of the data, these steps are performed in the reverse sequence in order to obtain the original data packet. Once the original packet is formed, it can be sent through existing wire-line networks. During one M-ES transmission burst, a fixed number of Reed-Solomon blocks, set by the service provider, are transmitted over the airlink (64 is the default value). However, the number of blocks formed from one data packet is dependent on the size of the NPDU the M-ES's application is sending. CDPD's raw data rate is 19.2 kilobits per second (kbps), but is actually more like 9.6 kbps because of the large amount of overhead it transmits along with the data.

The airlink is realized through frequency modulation of the data bit stream over one of the 800 MHz cellular channels described earlier. CDPD uses Gaussian Minimum Shift Keying (GMSK) for modulation because of its spectral efficiency and noteworthy performance in mobile channels where noise and fading are prominent.

1.4.3 Channel Access

An M-ES can access the reverse channel using a slotted non-persistent digital-sense multiple-access with collision detection (DSMA/CD) method. Any M-ES wishing to transmit first senses the forward channel stream for indicators called Busy/Idle flags which allow it to determine if the reverse channel is Busy or Idle. If the channel is Busy, the M-ES will wait or defer for a random entrance delay interval before it tries to access the channel again. The delay interval corresponds to a multiple of the time interval between Busy/Idle flags (60 bits). This represents the collision interval for the random access DSMA/CD Medium Access Control mechanism and is referred to as a microslot. In other words, the random entrance delay corresponds to the number of microslots delay before the channel status is sensed again by the M-ES. Each M-ES performs this process

independently, providing the slotted non-persistent aspect of DSMA.

If the Busy/Idle flag on the forward channel stream is sensed as Idle, the M-ES initiates a transmission within 8 bit times (416.7 microseconds) of the last bit of an Idle flag. Upon detecting the presence of a reverse channel transmission, the MDBS sets the Busy/ Idle flag to Busy, indicating to other M-ESs that the reverse channel is now occupied with a transmission from another M-ES. The transmitting M-ES begins by sending a dotting sequence and synchronization word before a continuous data stream, in the form of Reed-Solomon blocks, begins.

Having gained access to the reverse channel, continued access to the reverse channel is controlled by an indicator on the forward channel called the Decode Status flag. As Reed-Solomon data blocks are received by the MDBS, the status of the Decode Status flag is set to indicate the situation of the decoding procedure. If the decoding procedure was successful (the received block's errors were correctable), the M-ES continues transmission until all blocks have been transmitted or a decode failure occurs. If the decoding procedure was unsuccessful, the M-ES ceases transmission immediately and attempts to regain access to the channel after an appropriate delay time. The Decode Status flag is also used for collision detection. If two M-ESs transmitting at once collide trying to access the same reverse channel, the MDBS detects the collision and will indicate a Decode Status failure prompting both M-ESs to back off and retry later.

1.5 Strengths of CDPD

The main strength of CDPD lies in its packet switched capabilities and connectionless orientation as compared to circuit-switched techniques which send data over a continuous connection. With CDPD, the interconnection of all service providers (local cellular carriers) allows seamless packet data services to be available to every CDPD customer. However, with circuit-switching, customer mobility is usually restricted to the cellular

switch (MTSO) which means when moving to a new service area, the user becomes disconnected from the cellular network and must reestablish a connection for continued communications.

Another advantage is that CDPD uses less power than circuit-switching. When a device uses circuit-switching to send data, it needs to ramp up power and stay at a high level until all of the data is sent successfully. CDPD sends data packets in short bursts, so power only needs to ramp up for short intervals. Figure 1-4 shows that the result is less average power used. CDPD also has a "sleep" mode which allows the device to conserve

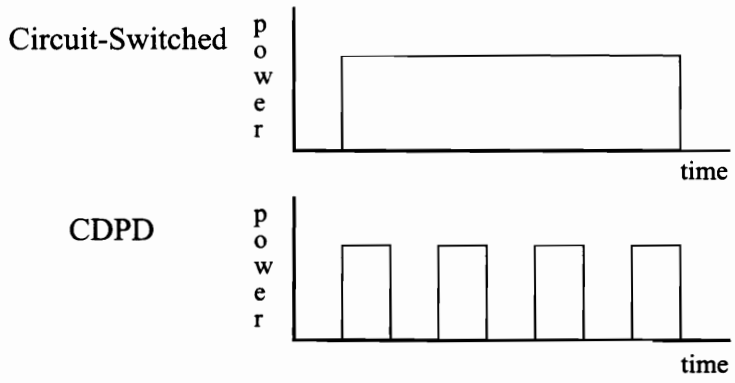

Figure 1-4: Average Power Usage [Puk94]

power when not currently being used, without having to log off the network. This translates to longer battery life for mobile computing devices using CDPD technology.

Circuit-switched data is also unsecured and susceptible to casual eavesdropping by a third party, just as a cellular voice call is. CDPD uses an encryption technique to prevent an outside source from receiving the transmitted data (barring multicast or broadcast modes).

CDPD is also an attractive choice for cellular carriers because they can leverage their existing resources. Since they already have engineering, customer service, and sales personnel in place, they only have to hire and train relatively few new people and set up a

few new systems. This translates into a significant cost savings.

1.6 CDPD Applications

CDPD is ideal for short transactions and can be used in transaction, batch, and broadcast/multicast applications.

Transaction applications provide communication between two network users and usually consists of an inquiry and a response message. These types of services may include credit card verification, vehicle dispatch, inventory control, emergency services, bi-directional paging, telemetry, and electronic mail.

Batch type applications provide subscribers a means to transmit data in one transaction allowing buffered, or saved, data to be transmitted entirely at a convenient time for the mobile users. This includes file transfers in which complete files can be copied from an external system to a mobile subscriber's system, or vice versa, using a file transfer application (e.g. FTP). Statistical information transfers also fall into this category where telemetry devices such as utility meters recording less critical information can transmit data during non-peak evening hours to save money on transaction costs.

Broadcast services would send messages to a large number of people in a specific geographical location. These messages are not acknowledged but may be sent several times to increase the probability of reception. Any information that can be sent over broadcast radio can be delivered using CDPD such as international news, local date and time, weather advisories, traffic advisories, and advertising.

Multicasting is a point-to-multipoint, one-way unacknowledged message transfer service to a particular group of subscribers. The service would send the message to all members of a multicast group regardless of their current location. This would include Information Service Subscriptions in which a service provider collects information and sells it on an inquiry basis to subscribers. Such information could include stock quotes,

want ads, or recreation information. Multicast may also include Private Bulletin Boards in which a mobile work force or business office could communicate with its employees.

Because CDPD is an integrated technology and can be used in a large variety of applications, it has also become a major player in the development of the Intelligent Transportation System's (ITS) physical architecture [Taylor95].

Cellular carriers must still work with customers to decide which applications are best suited for circuit switching and those best suited for packet switching. The industry consensus seems to have set the file-size dividing line at about 20 kilobytes, using circuit switching for larger files and packet switching for shorter ones. Table 1-1 shows the average sizes of different file types along with their preferred method of transfer [Stew95].

Table 1-1: Transmission Preferences For Different File Types

Data File Type	Size (bytes)	Preference
Faxes (per page)	20,000	Circuit
Compressed picture images	50,000 to 350,000	Circuit
Typical spreadsheet	20,000	Circuit
Typical word processing	15,000	Circuit
E-mail with attachment	20,000	Circuit
POS credit verification	90 to 130	Packet
E-mail without attachment	200	Packet
Dispatch	50	Packet
Messaging	100	Packet
Financial/information access	200	Packet
On-line access	200	Packet

The time lag between the introduction of a standard and the availability of new equipment has traditionally prolonged the installation of a new standard. However, this is

not the case for CDPD, a tribute to the nonproprietary openness of the specification.
The cost of CDPD is still a bit uncertain. Although the cellular companies seem quiet on the subject, initial costs are estimated to range from $35 to $45 for a monthly subscriber fee [Stew95]. Currently GTE Mobilenet has an activation charge of $45 in its Richmond, Virginia coverage area with tiered monthly rates ranging from $.12 / kilobyte to $.19 / kilobyte depending on the subscriber's plan [Puk94].

In general, CDPD has a lot to offer. First it can be deployed at practically every cell site in the nation, second, it is unobtrusive to the analog cellular phone network, third, because it is a packet switched network, it uses the OSI model and familiar suites and protocols, such as Transmission Control Protocol/Internet Protocol (TCP/IP) for data transmission.

CDPD now has its own trade association called the CDPD Forum Inc. The goals of the forum are to enhance and evolve the standard and specifications, ensure seamless interoperability, encourage and support hardware and software developers to build CDPD products, and promote widespread acceptance of CDPD technology in the marketplace [CDPDW95]. As CDPD roll out begins and its applications grow, we may soon see it become a major part of the cellular industry.

1.7 Research Objectives

Much of what has been published on CDPD focuses mainly on capacity and throughput issues and how to improve them [Jacobs94] [Jacobs95] [Taylor95]. These topics address the proportion of mobility management traffic arising form cell changes and its consumption of available bandwidth as well as the effects of channel hopping on throughput of the air interface. This had led to results citing the use of wideband receivers over narrowband receivers at base stations for channel monitoring and the suggestion of using an adaptive data rate technique to improve the system throughput.

The motivation for this research is to simulate and investigate the performance of the CDPD signal structure over the airlink in different channel environments. It is unclear how much of this type of work has previously been performed, but the work that has been done has taken place in industry and is proprietary information of the companies - this work is intended to make that information publicly available. This research will also compare the performance of two different receiver designs in the demodulation of the CDPD GMSK signal.

Chapter 2 delves deeper into the CDPD signal structure across the airlink for both the forward and reverse channels. Chapter 3 introduces modeling techniques using the Digital Signal Processing (DSP) software Signal Processing Workstation (SPW) and also explains the different aspects of the receiver designs. Results from the simulations are presented in Chapter 4 and a discussion of the simulation results along with conclusions are found in Chapter 5.

Appendix A contains information on the location of files that were created in the simulation of the CDPD system, naming convention for those files and instructions on loading and executing a simulation in SPW. It also explains the contents of all data files, input and output, used during simulation.

Chapter 2

The CDPD Signal Format

The basic unit of transmission on both the forward and reverse channel stream is a block of 378 bits. Transmissions consist of a burst containing an integral number of blocks, interleaved with various control flags and synchronization words that are detailed in following sections.

2.1 Forward Channel Block Structure

2.1.1 Reed-Solomon Encoding

Any time data is being transmitted, there is a chance that noise or other interference will cause the data to become corrupted. However, error correction methods can help compensate for this corruption by transmitting extra bits which contain redundant information. CDPD uses the Reed-Solomon forward error correction (FEC) method to send data over the forward and reverse channels. FEC improves the CDPD data transmission performance over a noisy airlink by avoiding the process of extensive re-transmission in the case that data is corrupted.

Each forward channel block is created using a systematic (63,47) Reed-Solomon code generated over the Galois Field GF(64), yielding a codeword based on six-bit symbols. For each Reed-Solomon block, there are 47 symbols of user data and 16 symbols of redundant data, called parity symbols, for a total of 63 symbols, hence the (63,47) name. Therefore, 282 bits of user data is encoded into a total of 378 bits for transmission. In a systematic Reed-Solomon code, the 282 bit information field after encoding is identical to

the 282 bits prior to encoding. Figure 2-1 illustrates one Reed-Solomon FEC data block.

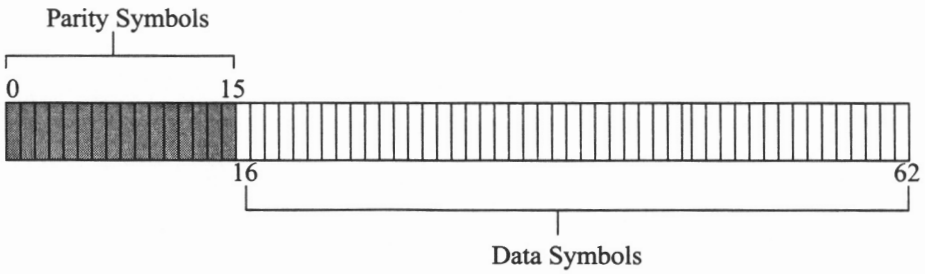

Figure 2-1: Reed-Solomon Block Structure

For encoding purposes, the bits in the transmission block can be considered to form a sequence of 63 six-bit Reed-Solomon code symbols $\{s_i\}$. These symbols are transmitted in sequential order from s_{62} to s_0 with the least significant bit of each symbol transmitted first. The information bits are contained in code symbols s_{62} to s_{16}, and the Reed-Solomon parity bits are contained in code symbols s_{15} to s_0. [Reed60], [Lin83] and [Berl87] give a detailed overview of the mathematics and theory in designing Reed-Solomon codes. What follows are some of the important characteristics of the CDPD (63,47) Reed-Solomon code.

The Reed-Solomon parity symbols are generated by using the generator polynomial:

$$g(x) = (x + a^1)(x + a^2).....(x + a^{16}) \qquad (2 - 1)$$

where a^1 is the primitive field element [010000] under the irreducible polynomial:

$$x^6 + x + 1 \qquad (2 - 2)$$

The Reed-Solomon parity symbols are found from the coefficients of the remainder poly-

nomial:

$$r(x) = s_{15}x^{15} + \ldots\ldots + s_1x^1 + s_0 \qquad (2 - 3)$$

which is formed as a result of dividing the shifted message polynomial:

$$x^{16}m(x) = s_{62}x^{62} + \ldots\ldots + s_{16}x^{16} \qquad (2 - 4)$$

by g(x) [CDPDS95].

A (63,47) Reed-Solomon error correcting code can correct up to eight symbol errors in a block, but the number of symbols which are actually corrected is implementation dependent. An implementation correcting only seven symbol errors leaves room for the detection of one symbol error and the use of an automatic repeat request (ARQ) scheme for the retransmission of an unsuccessfully decoded block.

The most common measure of performance for any error correction code is the estimated probability of transmission error. Since block codes act on symbols, an important parameter is the channel symbol error rate, P_{se}. This can be used to determine the probability of an uncorrectable error, P_{ue}.

An expression for the probability of an uncorrectable error in a block is given by [AHA95]:

$$P_{ue} = 1 - \sum_{i=0}^{t} \binom{n}{i} (P_{se})^i (1 - P_{se})^{n-i} \qquad (2 - 5)$$

where n is the number of symbols per code block and t is the number of correctable symbol errors. The bit error rate, P_b, rather than the symbol error rate may be known for a given channel. Under the assumption of purely random errors, they are related by:

$$P_{se} = 1-(1-P_b)^m \qquad (2-6)$$

where m is the number of bits per symbol, in our case 6. For more complicated, less random error characteristics, the P_{se} needs to be determined on a case by case basis. In general, Reed-Solomon codes perform better when most errors are concentrated within a few symbols. The formułas presented here generally predict larger error probabilities than will be encountered with correlated or burst type errors. Figure 2-2 shows a performance curve for the (63,47) Reed-Solomon code when decoding different numbers of symbol errors. An important item to notice is for error rates below $P_{se} = 10^{-2}$, the performance curve hasa very steep slope. The 10^{-2} value forms a threshold on the P_{se} for the satisfactory performance of the code. This steep slope is preferred for data communications because large improvements in output P_{ue} are possible for small improvements in input P_{se}.

When a block code fails to correct a block, the integrity of the entire data block can be lost due to only a few errors. Because of this, standard bit error rate (BER) curves which are used to analyze independent bit errors can be misleading. For this reason, another performance measure is useful, the Corrected Bit Error Rate (CBER). The CBER is the reciprocal of the expected number of correct bits between errors and is given by [AHA95]:

$$CBER = \frac{P_{ue}}{n \cdot m}$$

where n is the total number of symbols per block (63) and m is the number of bits per symbol (6). The data in figure 2-2 converted to CBER is shown in Figure 2-3.

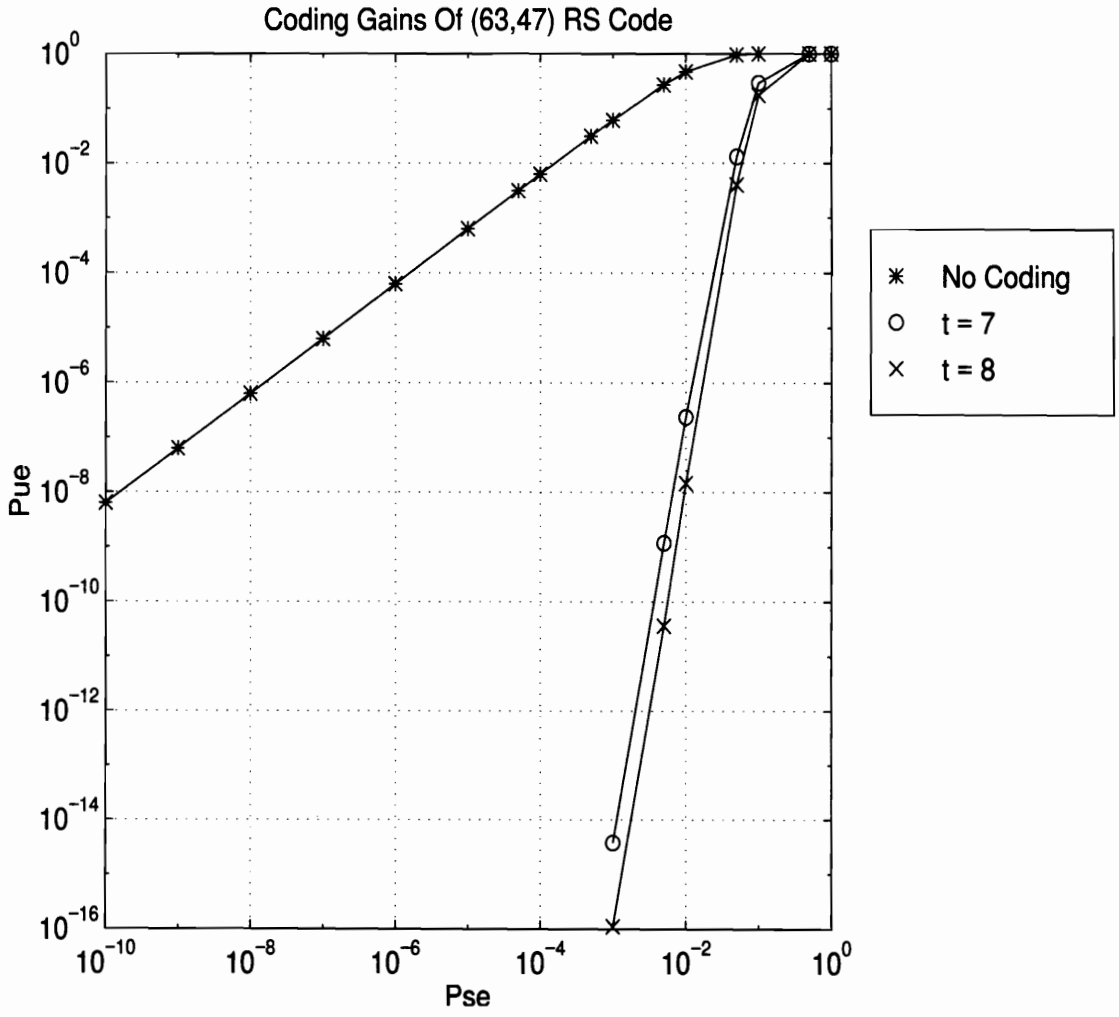

Figure 2-2: Performance Of (63,47) RS Code

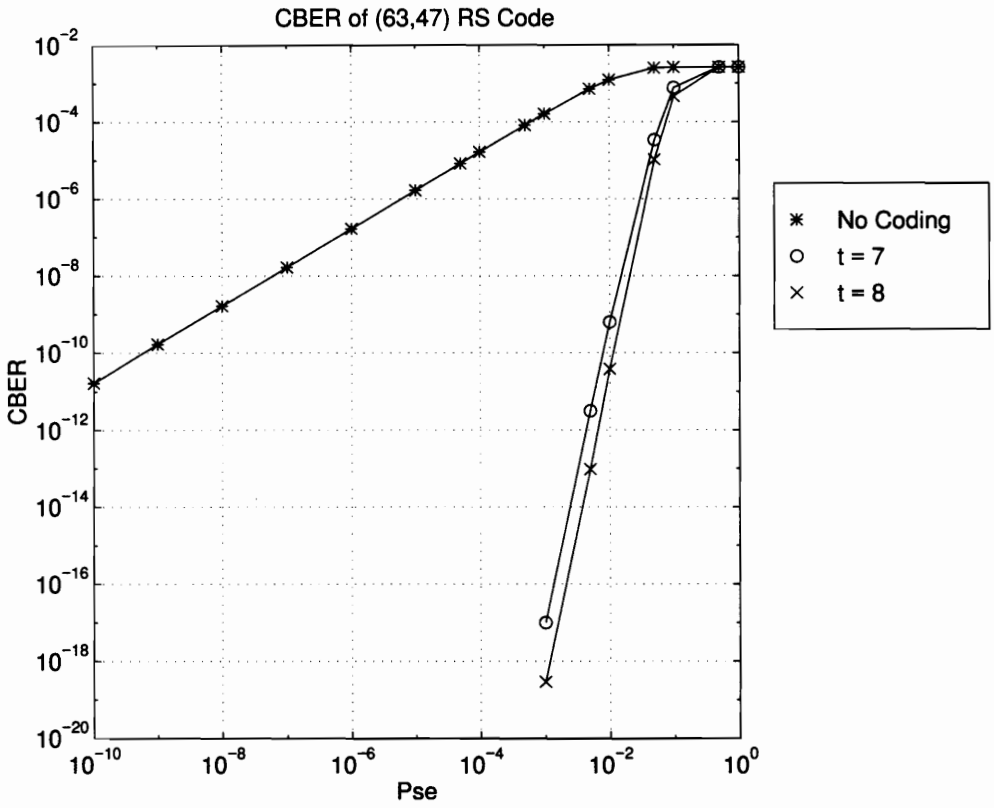

Figure 2-3: Performance Of (63,47) RS Code In Terms Of CBER

Figure 2-3 shows that when correcting seven symbol errors, the CBER is 10^{-17} when $P_{se} = 10^{-3}$ for the (63,47) RS code. This means that if one in one thousand symbols are in error, there will be an average of 10^{17} bits between errors after decoding.

2.1.2 Pseudo-Random Number (PN) Coverage

After Reed-Solomon encoding and prior to transmission, the information and parity bits in each block are XOR-ed with a pseudo-random number sequence. In a systematic Reed-Solomon code, there is a possibility that long strings of binary 1's and 0's could exist. Certain types of demodulators may not be able to track these long strings of 1's and

0's. For this reason, the PN sequence is exclusive or'd with each 378-bit block to maximize the likelihood of bit transitions in the block during transmission. Each block is exclusive or'd with the same PN sequence after reception and before Reed-Solomon decoding to remove the PN sequence.

The PN sequence is generated under the generator polynomial:

$$g(D) = D^9 + D^8 + D^5 + D^4 + 1 \qquad (2 - 7)$$

and is initialized every 378 bits with the binary value 111000101. A shift register implementation is shown in Figure 2-4 below [CDPDS95].

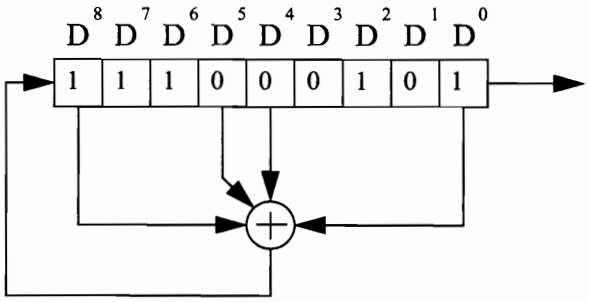

Figure 2-4: Shift Register Implementation Of PN Sequence Generator

2.1.3 Control Symbols

The basic format for forward channel transmissions is a 378 bit (63,47) Reed-Solomon codeword that is interleaved with a forward synchronization word and control flags as shown in Figure 2-5. The 282 data bits are first encoded using the forward error correcting Reed-Solomon code to form a 378 bit block made up of 63 six-bit code symbols. The RS block is then exclusive or'd with the PN Sequence. Seven control symbols are then inserted before Reed-Solomon code symbols s_{62}, s_{53}, s_{44}, s_{35}, s_{26}, s_{17}, and s_8 in

each block.

Each control symbol is made up of 5 Busy/Idle Status flags and a Decode Status flag as shown in Table 2-1. Prior to transmission, the 5 Busy/Idle Status bits are Exclusive-Or'd with one five bit group of the forward synchronization word as shown in Figure 2-5. The sixth bit is one of the bits of the Decode Status flag. The combination of the Busy/Idle flag and one bit of the Decode Status flag makes up the Control Symbol.

Table 2-1: Control Symbol Structure

Bit	6	5	4	3	2	1
Value	Decode Status	Busy/Idle Status				

The Busy/Idle Status flag is a 5-bit sequence used to signal the status of the reverse channel as shown in Table 2-2. Since each flag is exclusive or'd with five bits from the forward synchronization word, the actual value of the flag is affected by its position in the block.

Table 2-2: Busy/Idle Status Flag Encoding

State	Binary Encoded Value
Channel Busy	00000
Cannel Idle	11111

Because the MDBS is unable to distinguish between random or burst errors on the radio channel, and errors due to collisions of reverse channel transmissions from two or more MESs, a single status flag is used to cover both classes of errors. This flag is the Decode Status flag. The Decode Status flag is a seven bit sequence that signals whether the MDBS was able to decode the proceeding block received on the reverse channel in the current burst. The coding

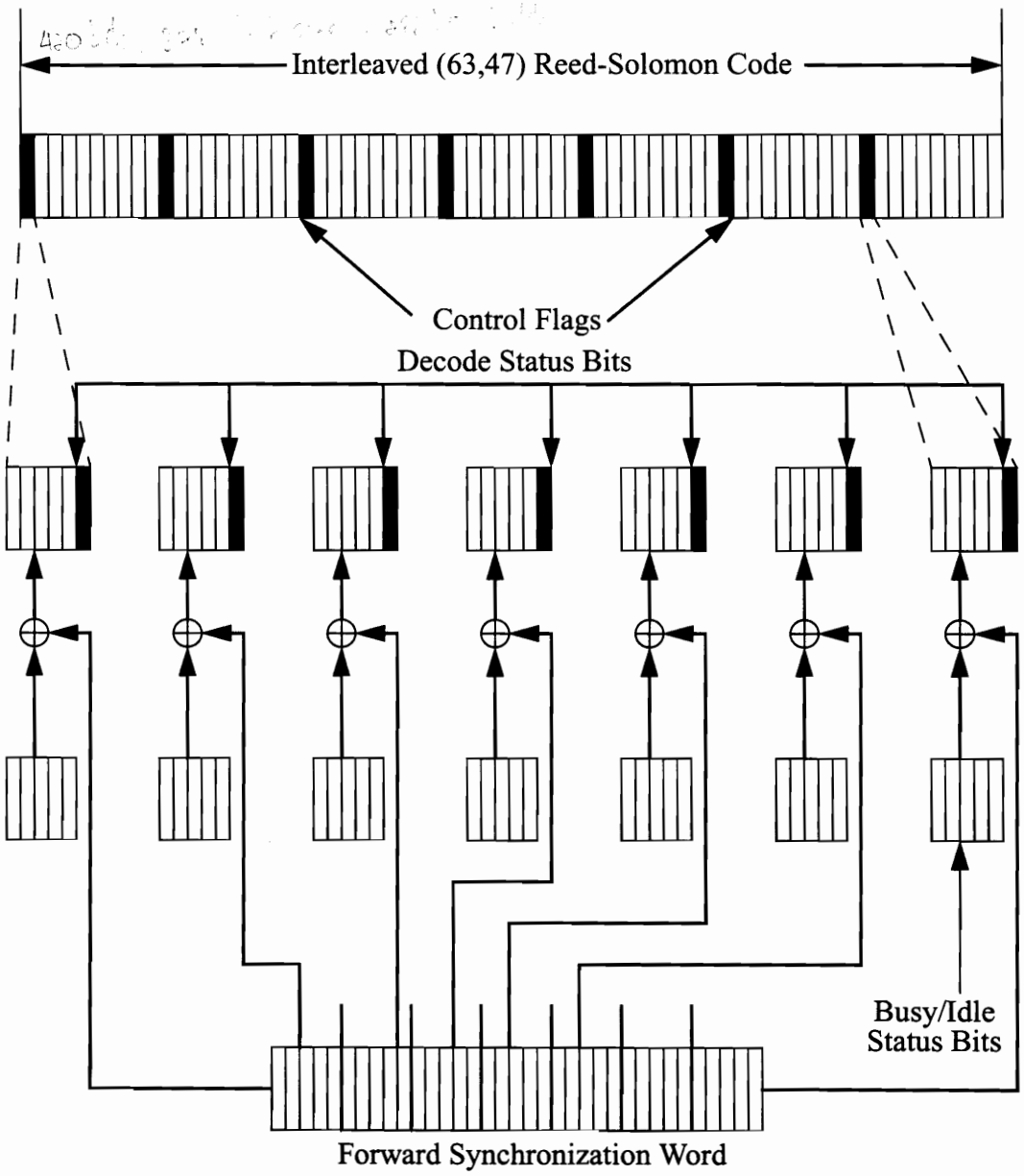

Figure 2-5: Foward Channel Transmission Structure [CDPDS95]

of this flag is shown in Table 2-3.

Table 2-3: Decode Status Flag Encoding

State	Binary Encoded Value
Decode Success	0000000
Decode Failure	1111111

The bits of the Decode Status flag are transmitted consecutively with one bit of the flag immediately following each Busy/Idle flag as shown in Figure 2-5. Once the Decode Status flag has been set to "0" by the MDBS after a decode success, all subsequent Decode Status bits are also set to "0" until a decode failure is signalled. Likewise, once the Decode Status bit has been set to "1" after a decode failure, all subsequent Decode Status bits are also set to "1" until a decode success is indicated.

2.1.4 Synchronization Word

The forward channel synchronization word is a 35-bit sequence that provides a reference marker within the forward channel bit stream to discriminate the reverse channel status flags and Reed-Solomon block boundaries. It also provides the timing reference for the reverse channel digital sense multiple access (DSMA) with collision detection (CD) microslot clock. The binary value of the forward synchronization word is, in order of bit transmission:

$$11101\ 00001\ 11000\ 00100\ 11001\ 01010\ 01111 \qquad (2 - 8)$$

The sequence is transmitted in seven groups of five bits, each group exclusive or'd with one 5-bit Busy/Idle flag. Each resultant 5-bit group is inserted before Reed-Solomon code symbols s_{62}, s_{53}, s_{44}, s_{35}, s_{26}, s_{17}, and s_8 in each forward channel block. Therefore, the actual value of the transmitted 5-bit group is affected by the current value of the Busy/Idle

status flag. Each transmitted 5-bit group will hold the value of the actual synchronization word or its complement.

2.2 Reverse Channel Format

2.2.1 RS Encoding and PN Sequence Coverage

The Reverse Channel transmission blocks are created in the exact same manner as the Forward Channel blocks. 282 information bits are encoded using the (63,47) RS code described in the section 2.1.1. The Reverse Channel RS blocks also undergo the same PN Sequence coverage as described in section 2.1.2.

2.2.2 Continuity Indicator

After RS encoding and PN Sequence coverage, the reverse channel RS block is interleaved with a Continuity Indicator. The Continuity Indicator is a seven bit sequence that signals whether the reverse transmission burst is complete and is encoded as shown in Table 2-4.

Table 2-4: Continuity Indicator Encoding

State	Binary Encoded Value
Final Block (End Of Transmission)	0000000
More Blocks	1111111

The bits of the Continuity Indicator are interleaved with the Reed-Solomon block, one bit every nine 6-bit symbols as shown in Figure 2-6. One bit of the Continuity Indicator is inserted before Reed-Solomon code symbols s_{62}, s_{53}, s_{44}, s_{35}, s_{26}, s_{17}, and s_8 in each

reverse channel block.

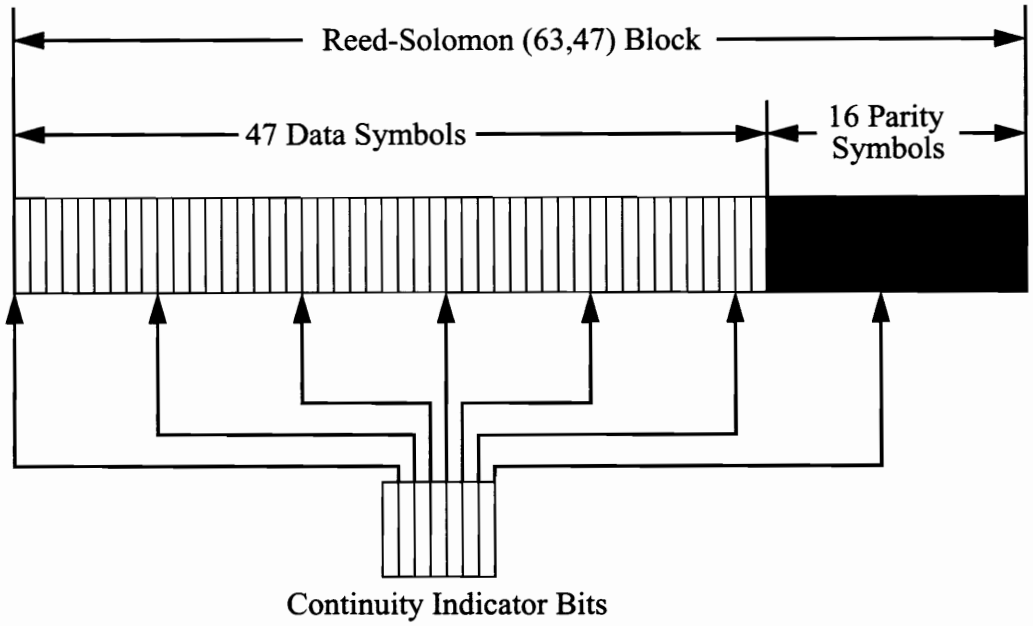

Figure 2-6: Reverse Channel Transmission Structure [CDPDS95]

2.2.3 Dotting Sequence and Synchronization Word

The reverse channel burst begins with a 38-bit dotting sequence, which is used by the MDBS for transmission burst detection and bit timing recovery. The binary value of the dotting sequence is, in bit transmission order:

1010 1010 1010 1010 1010 1010 1010 1010 1010 10 (2 - 9)

The dotting sequence is immediately followed by a 22-bit reverse synchronization word that is used by the MDBS to obtain block synchronization with the M-ES. The binary value of the reverse synchronization word, in bit transmission order, is:

1011 1011 0101 1001 1100 00 (2 - 10)

2.3 Gaussian Minimum Shift Keying (GMSK)

CDPD uses Gaussian filtered minimum shift keying (GMSK) for modulation which has been found to be a spectrum-efficient form of digital modulation for mobile radio channels [Murota81]. GMSK is a form of minimum shift keying (MSK), which is continuous phase binary digital FM with a modulation index of 0.5 and has the following properties: a constant envelope, a relatively narrow bandwidth, and the capability of coherent detection. However, MSK does not satisfy the requirements with respect to out-of-band radiation for mobile radio, so premodulation filtering must be used.

The GMSK RF signal has a constant envelope and the phase varies in a continuous manner (Continuous Phase Modulation [CPM]). CPM signals can be described by:

$$s(t) = A \cdot \cos\left(\omega_0 t + 2\pi \cdot \sum_{i=0}^{n} \alpha_i \cdot h \cdot q(t - iT) \right) \qquad (2 - 11)$$

where α_i are the binary symbols with values +1 and -1 and h is the modulation index. The function $q()$ is the phase response function. CPM schemes are denoted by their phase response function or by its derivative $g()$, the frequency response function.

With GMSK, the digital binary data is filtered by a Gaussian low-pass filter before modulation by the FM modulator. This provides a narrow bandwidth to suppress high frequency components and a lower overshoot impulse response to protect against excessive instantaneous frequency deviation [Murota81]. The output power spectrum can be controlled by varying the bandwidth of the Gaussian LPF. Denoting B as the 3-dB bandwidth of the Gaussian LPF and T as the data period, the bandwidth time product, BT, gives a normalized quantity of filter throughput. Different filter shapes for varying BT products

are shown in Figure 2-7.

This narrowband spectrum is achieved at the sacrifice of introducing severe intersymbol interference (ISI) into the baseband waveform of the FM modulator input. Figure 2-7 shows that for decreasing BT products, the amount of ISI increases. The System Specification requires that the BT product for CDPD be 0.5 with a bit rate of 19.2 kbps, this implies a 3-dB filter bandwidth of 9600 Hz. Figure 2-8 shows a non-return to zero (NRZ) data stream with 5 samples/bit which has been Gaussian low-pass filtered with

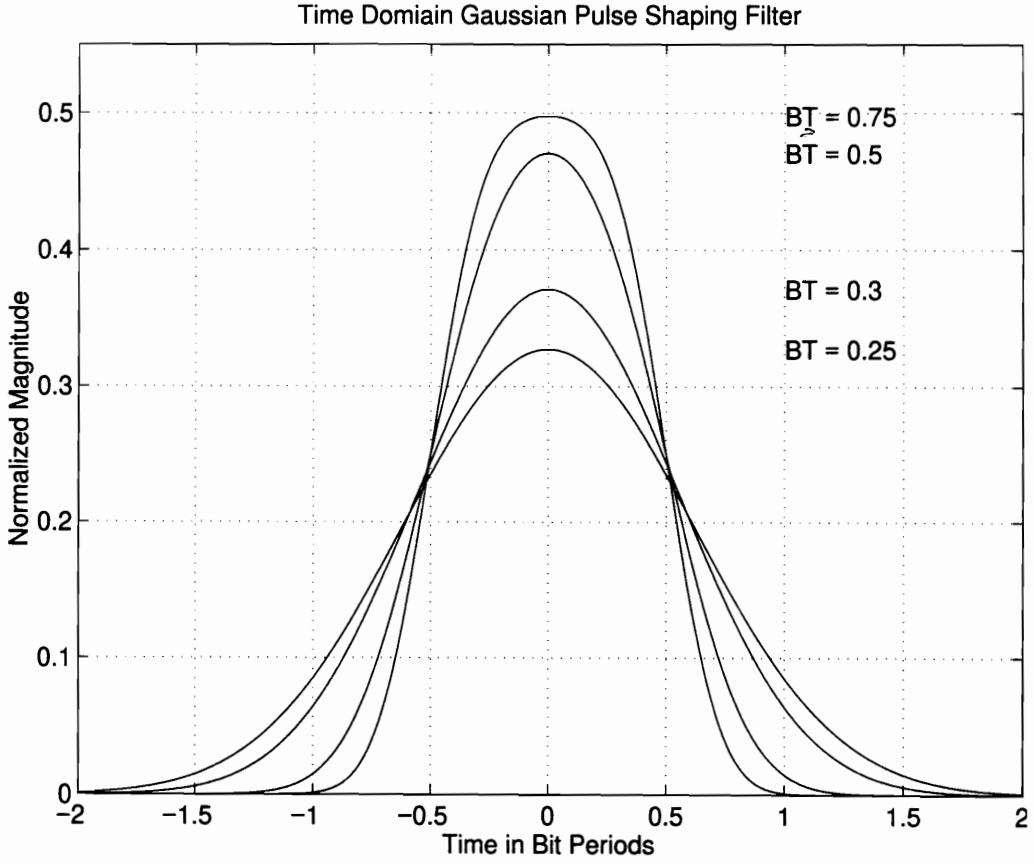

Figure 2-7: Gaussian Low-Pass Filter Shaping

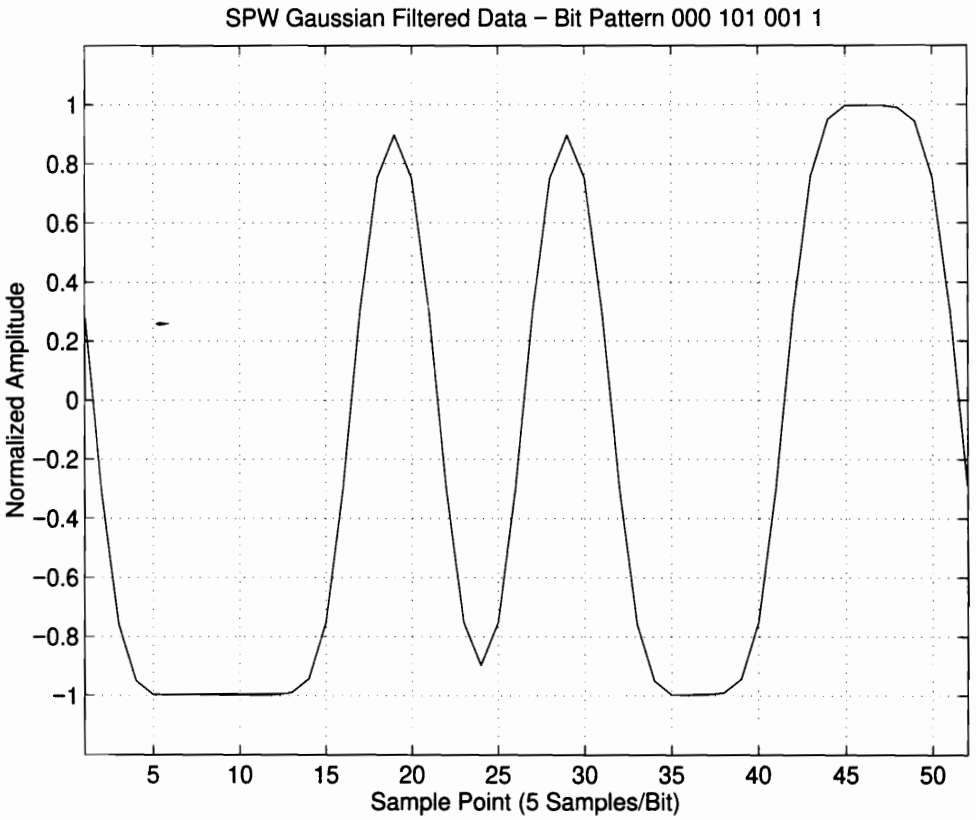

Figure 2-8: Gaussian Low Pass Filtered Data

a BT product of 0.5. Due to the ISI, the waveform only reaches a peak value when consecutive 1's or 0's appear in the bit stream.

The time domain pulse shaping filter for GMSK, which is the difference of two Gaussian filters, is defined as:

$$g(t) = \frac{1}{2T}\left[Q\left\{2\pi B\left(\frac{t-\frac{T}{2}}{\sqrt{\ln 2}}\right)\right\} - Q\left\{2\pi B\left(\frac{t+\frac{T}{2}}{\sqrt{\ln 2}}\right)\right\}\right] \qquad (2 - 12)$$

where

$$Q(t) = \int_{t}^{\infty} \left(\frac{1}{\sqrt{2\pi}} \right) e^{-\tau^2/2} d\tau \qquad (2 - 13)$$

In this definition T is the bit period and B is the filter bandwidth [CDPDS95].

Figures 2-9 and 2-10 show eye diagrams for the baseband GMSK signal with $BT = 0.5$ and $BT = 0.3$ respectively. The differences in eye openings due to the ISI can clearly been seen. GMSK is also used in GSM (Groupe Special Mobile) which is the major European telecommunications standard. GSM uses a BT product of 0.3, while CDPD uses a product of 0.5.

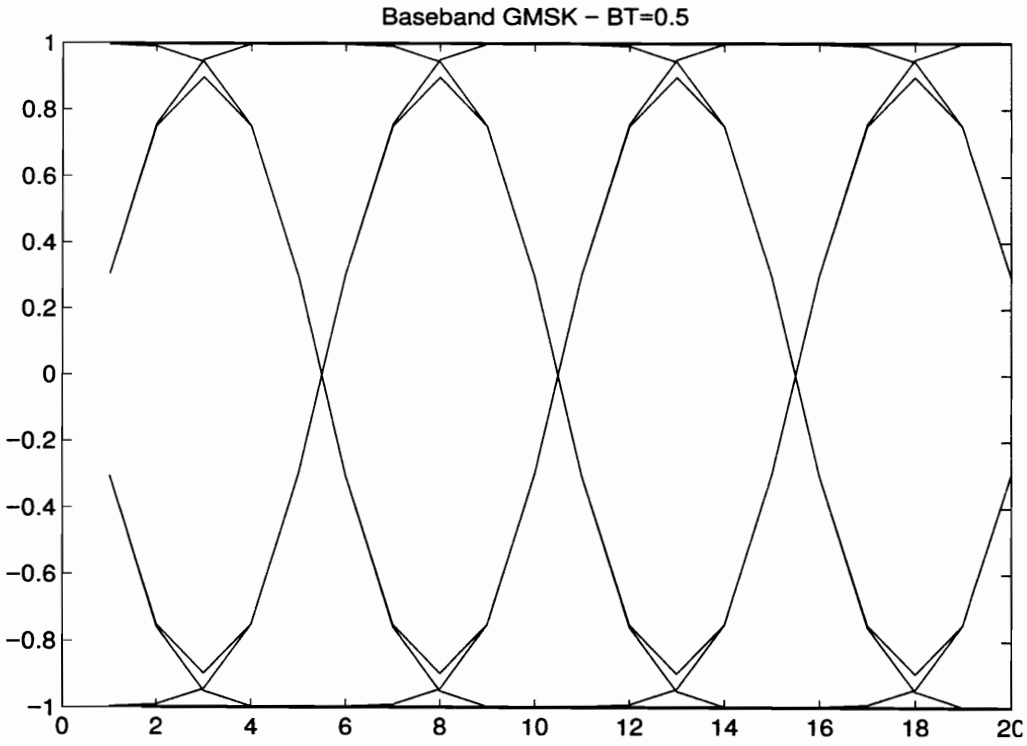

Figure 2-9: GMSK Eye Diagram, BT = 0.5

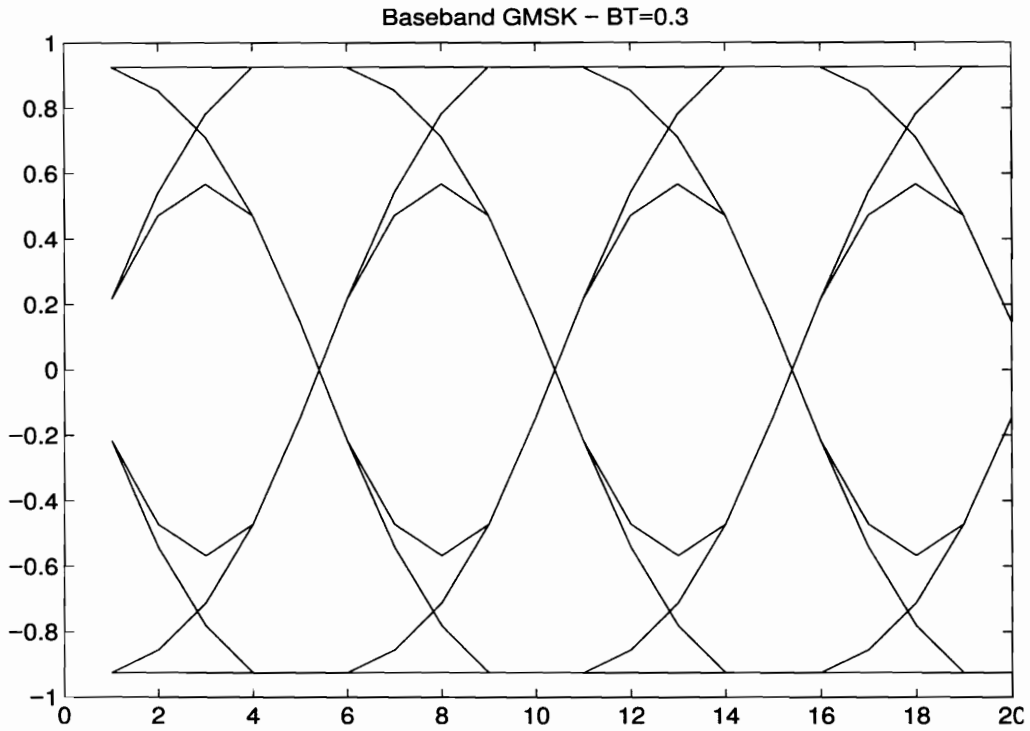

Figure 2-10: GMSK Eye Diagram, BT = 0.3

Chapter 3

System Modeling

3.1 Signal Processing Workstation (SPW)

This work was performed using the digital signal processing tool SPW, version 3.1, designed by Cadence Design Systems, Inc. SPW assumes that all systems, whether they are simple functional blocks, such as modulators, or entire communications links, can be described in a hierarchical block diagram form. To simulate a system, you must first construct a block diagram of the system by bringing existing models from the library to the screen and connecting them in the desired topology. This is done graphically in a way that is analogous to drawing block diagrams on a piece of paper. In this way, block diagrams of complex systems are constructed in a hierarchical fashion from the bottom up. In the event that a new function can't be implemented or constructed from the existing libraries, a new model can be graphically designed and linked to source code written in C or FORTRAN which will perform the desired function. This block can then be stored in SPW's database and used as any other library model.

Hierarchical design is an important concept in SPW. A number of blocks can be grouped together to form a larger block that performs a specific function. A new graphical symbol can be created for this new function, and the blocks which make up this new function are linked to the symbol as its *detail*. In this way, new blocks can also be added to SPW's database and used as any other library model. This allows for graphical designing at a high level of functionality.

The time functions used in simulating communications systems are often carrier-modulated signals in bandpass systems. To sample these functions, SPW uses the fact that it is more efficient and simpler to sample lowpass than bandpass functions. This is based on the narrowband assumption that for bandpass systems the bandwidth is usually much smaller than the carrier frequency, and that a continuous signal is uniquely represented by a discrete model only if the sampling theorem is satisfied.

If the signal spectrum is contained in the band $f_c - B/2 \le f \le f_c + B/2$, a naive interpretation of the sampling theorem might indicate that the sampling frequency would have to be on the order of $2f_c + B$. The sampling frequency needs to be only on the order of B, which is twice the highest frequency in the information signal. SPW analyzes and simulates carrier modulated signals and systems as if they were lowpass. The technique to implement this idea is the complex envelope method and is central to simulation [SPW94].

Any physical bandpass waveform can be represented by

$$v(t) = Re\{g(t)e^{j\omega_c t}\} \qquad (3 - 1)$$

where $Re\{\delta\}$ denotes the real part of δ, $g(t)$ is the complex envelope of $v(t)$, and f_c is the associated carrier frequency (hertz) where $\omega_c = 2\pi f$. Two other equivalent representations are

$$v(t) = R(t)\cos[\omega_c t + \phi(t)] \qquad (3 - 2)$$

and

$$v(t) = x(t)\cos\omega_c t - y(t)\sin\omega_c t \qquad (3 - 3)$$

where

- $g(t) = x(t) + jy(t) = |g(t)|e^{j\angle g(t)} \equiv R(t)e^{j\phi(t)}$
- $x(t) = Re\{g(t)\} \equiv R(t)\cos\phi(t)$
- $y(t) = Im\{g(t)\} \equiv R(t)\sin\phi(t)$
- $R(t) \equiv \sqrt{x^2(t) + y^2(t)}$ is the amplitude modulation
- $\phi(t) \equiv \text{atan}\left(\frac{y(t)}{x(t)}\right)$ is the phase modulation

The waveforms $g(t)$, $x(t)$, $y(t)$, $R(t)$, and $\phi(t)$ are all baseband waveforms and, except for $g(t)$, they are all real waveforms. SPW can treat the envelope $g(t)$ as an equivalent lowpass signal during simulation [Couch93].

3.2 Transmitter Model

The block diagram for the CDPD transmitter is shown in Figure 3-1. A random data file was created in SPW's Signal Calculator with one sample per bit and linked to a SPW block for simulation data. Vector blocks are used for data manipulation until the filtering and modulation stages. A vector of 282 bits is sent from the Data Generation block to a block which performs the Reed-Solomon encoding. The Reed-Solomon block encodes the data and outputs a 378 bit vector to the PN Sequence Coverage block where the bits are exclusive or'd with a pseudo-random sequence according to the system specification.

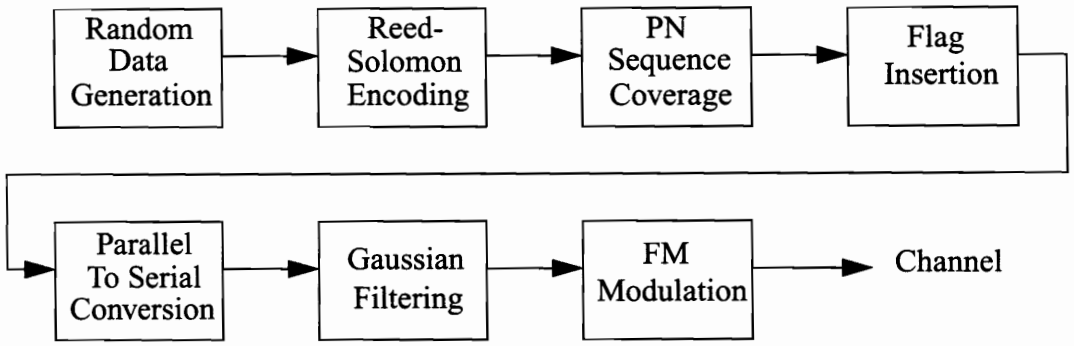

Figure 3-1: Transmitter Block Diagram

The 378 bit output of the PN Sequence Coverage block is then passed to a Flag Insertion block where the Reed-Solomon block is interleaved with system flags. On the forward channel, this block inserts 7 six-bit Control Flags giving an output of 420 bits. On the reverse channel the block inserts 7 one-bit Continuity Indicators giving an output of 385 bits. The blocks of data are then converted to a serial bit stream at five samples per bit and Gaussian filtered before FM modulation.

Both the forward and reverse channel transmitter are structured in very much the same way. The only difference between the two lies in the fact that a reverse channel transmission burst begins with a dotting sequence followed by a synchronization word before sending interleaved Reed-Solomon blocks.

Simulations were run at different Eb/Nos until a total of 15 block errors were reached. Timing is used to ensure that the serial data stream is continuous from block to block during filtering, modulation, and transmission over the channel. Frequency hopping was not modeled in the simulation which have some effect on performance, but more on throughput and capacity than error rates.

3.3 Receiver Models

A basic block diagram of the receiver structure is shown in Figure 3-2. Data from the channel is demodulated and converted to vector form for processing. After extracting the flags from the Reed-Solomon block and removing the PN Sequence, the data is passed to a block which gauges the performance of the received data. The SPW Reed-Solomon decoder could only correct the maximum number of symbol errors possible by the code, in our case eight. But the system specification recommends that only seven symbols be

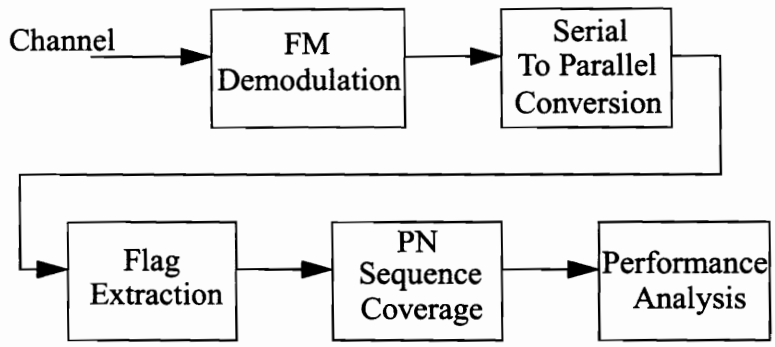

Figure 3-2: Receiver Block Diagram

corrected leaving room for the detection of one symbol error for retransmission requests. The performance analysis block actually does no decoding but compares the received block with the transmitted block. It receiver keeps track of bit errors and block errors for the cases of no coding and correcting seven symbol errors. It will also record the number of symbol errors per block, the total number of symbol errors and any errors in the synchronization words, interleaved flags, or dotting sequence.

The two methods used for demodulation are frequency discrimination and one-bit differential detection. Each method is explained further in the following sections.

3.3.1 Frequency Discrimination

The block diagram of a balanced frequency discriminator, is shown in Figure 3-3. Two tuned circuits are used to balance out the dc component when the input has a carrier frequency of f_c. They also provide an extended linear frequency-to-voltage conversion characteristic. SPW's FM Discriminator demodulates the GMSK signal from its complex envelope representation using two Butterworth lowpass filters while translating the signal spectrum to provide the required bandpass filtering.

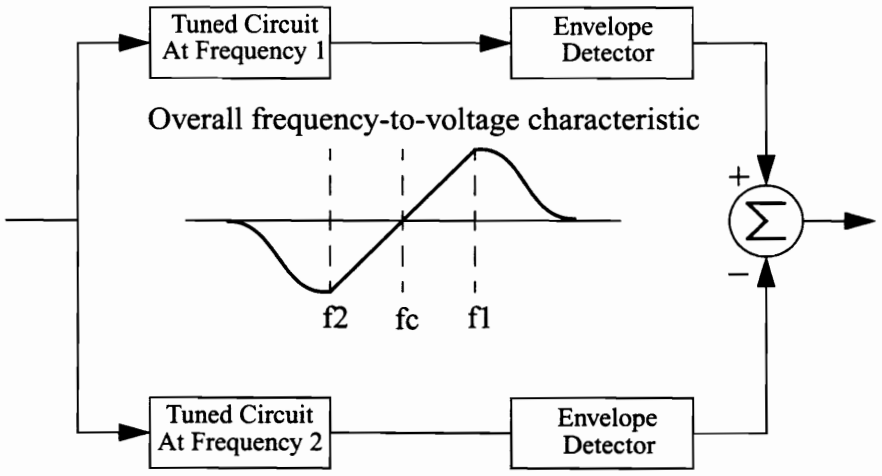

Figure 3-3: Frequency Discriminator Block Diagram

The output of the FM discriminator is then sent to an integrate and dump block for a bit decision. This block performs a Trapezoidal-approximation integral of the input signal over one bit period (5 samples). If the integral over the bit period is greater than zero, it is received as a "1". If the integral is less than or equal to zero, the bit is received as a "0". At this stage, once a decision has been made the number of samples per bit is once again reduced to 1.

3.3.2 One-Bit Differential Detection

Differential detection involves multiplying the received signal by a version of itself that is delayed by a symbol time T and phase shifted by $90°$. The block diagram of a conventional one-bit differential detector is illustrated in Figure 3-4.

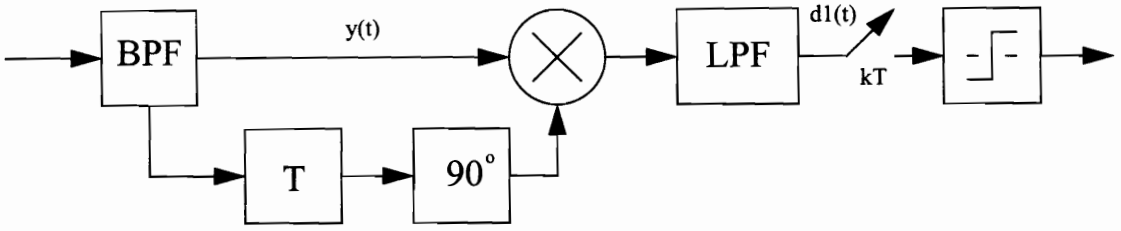

Figure 3-4: Block Diagram Of A One-Bit Differential Detector

Following the convention set forth in [Yong88], the signal at the output of the bandpass filter, y(t), can be represented as

$$y(t) = r(t)\cos(\omega_c t + \phi(t)) + n_c(t)\cos\omega_c t - n_s(t)\sin\omega_c t \qquad (3 - 4)$$

where $r(t)$ is the time-varying envelope of the signal, $\phi(t)$ is the distorted signal phase, and $n_c(t)$ and $n_s(t)$ are the in-phase and quadrature components of the narrowband noise, respectively.

The output of the one-bit detector, $d_1(t)$, is obtained by lowpass filtering the product of $y(t)$ and a T seconds delayed and $90°$ phase shifted version of itself giving

$$d_1(t) = r(t)r(t-T)\sin\left(k_m \sum_{j=-\infty}^{\infty} b_j \int_{(t-T)}^{t} g(\tau - jT)d\tau\right) + n_1(t) \qquad (3\text{ - }5)$$

where $n_1(t)$ lumps all the noise terms together and it is assumed that $\omega_c T = 2k\pi$ where k is an integer.

At the time instant kT, $d_1(t)$ has the following form

$$d_1(kT) = r(kT)r(kT-T)\sin\left(\sum_{j=-\infty}^{\infty} b_j \Theta_{k-j}\right) + n_1(kT) \qquad (3\text{ - }6)$$

where

$$\Theta_{k-j} = k_m \int_{(kT-t)}^{kT} g(\tau - jT)d\tau \qquad (3\text{ - }7)$$

The values of Θ_i for different $B_t T$ have been tabulated in Table 3-1. Here Θ_0 represents the signal with Θ_{-3}, Θ_{-2}, Θ_{-1}, Θ_1, Θ_2, and Θ_3 representing the ISI terms. For $|i| \geq 3$, Θ_i is negligible. This enables equation 3-6 to be written as

$$d_1(kT) = r(kT)r(kT-T)\sin(\Delta\Theta_k) + n_1(kT) \qquad (3\text{ - }8)$$

where

$$\Delta\Theta_k = b_{k+2}\Theta_{-2} + b_{k+1}\Theta_{-1} + b_k\Theta_0 + b_{k-1}\Theta_1 + b_{k-2}\Theta_2$$

Table 3-1: Phase Shifts For Signal, Θ_0 And ISI Terms, Θ_i

B_tT	Θ_{-3}	Θ_{-2}	Θ_{-1}	Θ_0	Θ_1	Θ_2	Θ_3
0.15	0.3	4.55	21.85	36.6	21.85	4.55	0.3
0.3	-	0.2	15.9	57.8	15.9	0.2	-
0.5	-	-	10.3	69.4	10.3	-	-
1.0	-	-	5.9	78.2	5.9	-	-
∞ (MSK)	-	-	-	90	-	-	-

For B_tT = 0.5, the differential phase angles, $\Delta\Theta_k$, corresponding to all possible input data combinations have been tabulated in Table 3-2. The diagrams in which all possible differential phase angles at the sampling instants (i.e. $\Delta\Theta_k$) are shown are referred to as phase-state diagrams. Using Table 3-2, the phase-state diagram of the one-bit detector for B_tT = 0.5 can be found and is shown in Figure 3-5.

Table 3-2: Differential Phase Angles Of The One-Bit Differential Detector, BT = 0.5

Bit Combinations			State	$\Delta\Theta_k$
b_{k-1}	b_k	b_{k+1}		(in degrees)
1	1	1	1	90
1	1	-1	2	69.4
-1	1	1	2	69.4
-1	1	-1	3	48
1	-1	1	4	-48
1	-1	-1	5	-69.4

Bit Combinations			State	$\Delta\Theta_k$
b_{k-1}	b_k	b_{k+1}		(in degrees)
-1	-1	1	5	-69.4
-1	-1	-1	6	-90

Figure 3-5 shows that the phase-states are symmetric with respect to the x-axis, consequently the corresponding eye diagram shown in Figure 3-6 is also symmetric. Also, the decision threshold is the x-axis. When the phase difference ($\Delta\Theta_k$) is above the x-axis, b_k is decoded as a "+1", otherwise b_k is decoded as a "-1". Or

$$b_k = \text{sgn}[d_1(kT)] \tag{3 - 9}$$

where $\text{sgn}[x] = 1$ for $x \geq 0$ and $\text{sgn}[x] = -1$ for $x < 0$. Recall that for one-bit differential detection a differential encoder is not used, therefore $a_k = b_k$.

From [Simon84] it is known that an optimum value of receiver B_rT product will exist for each B_tT product associated with the transmitter Gaussian pulse shaping filter. These optimum values are also a function of the level of bit error probability performance. Table 3-3 shows these values for bit error probabilities of 10^{-3} and 10^{-6} During simulations a receiver B_rT product of 1.10 is used since it is optimum for both bit error probabilities for a transmitting B_tT of 0.5.

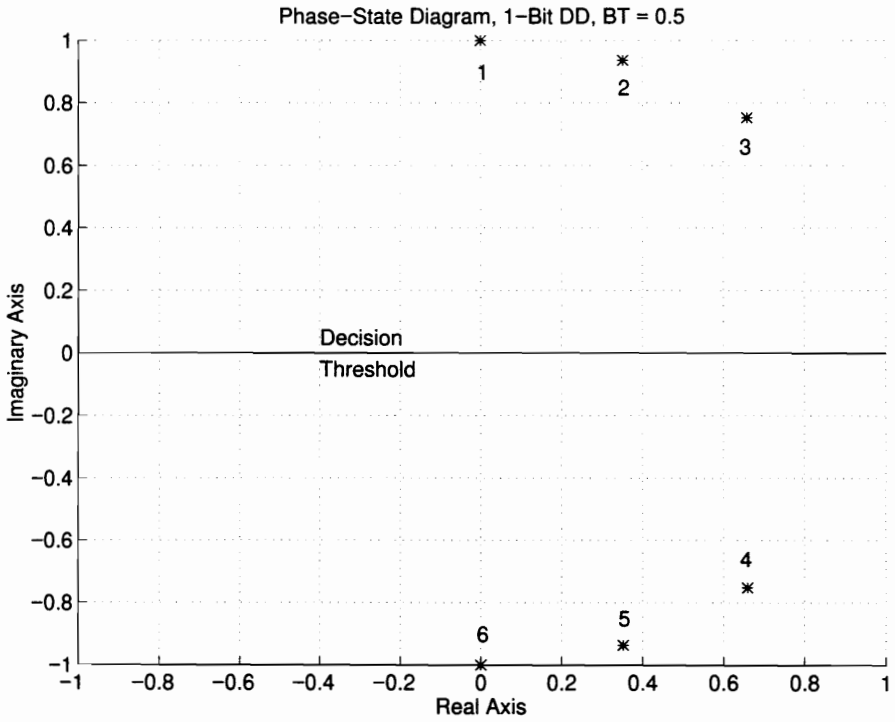

Figure 3-5: Phase-State Diagram, One-Bit DD, BT = 0.5

Table 3-3: .Optimum B_rT Products

Transmitting B_tT	Optimum Receiver B_rT	
	Pb = 10^{-3}	Pb = 10^{-6}
∞	1.00	1.15
1.0	1.05	1.15
0.5	1.10	1.10
0.4	1.10	1.15
0.32	1.20	1.20
0.25	1.40	1.45

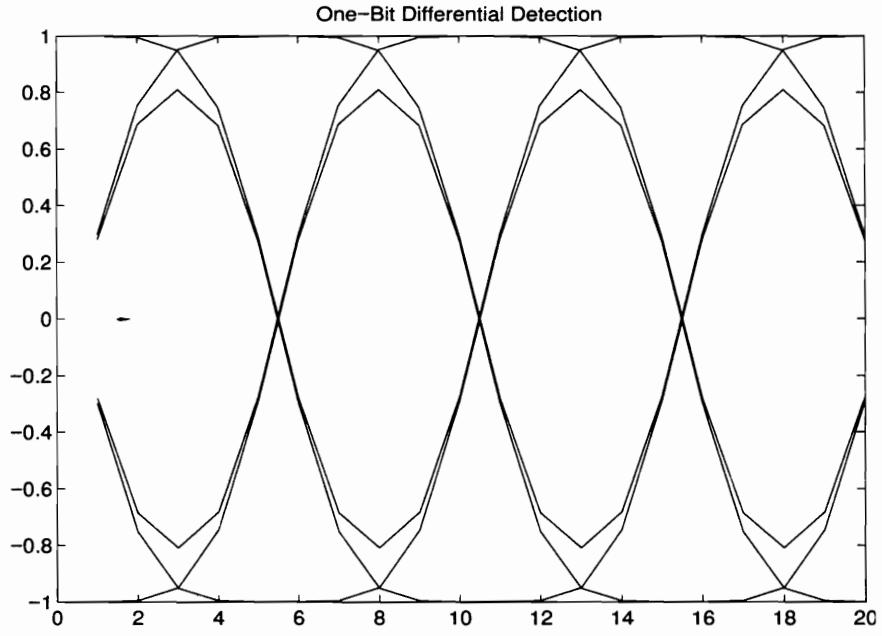

Figure 3-6: Eye Diagram Of One-Bit Differential Detector

3.4 Channel Models

3.4.1 Additive White Gaussian Noise (AWGN)

An SPW Complex White Noise block was used for the AWGN model. It generates complex Gaussian white noise in which the mean and variance can be specified as parameters. The mean of the noise is set to zero, while the variance is changed to yield different values of E_b/N_o. The complex output of this block was added to the complex output of the GMSK modulated signal before being sent to the receiver. The block diagram of the system in shown in Figure 3-7. This simulation was useful in verifying the simulation model against published works for uncoded GMSK with $BT = 0.5$ in Gaussian noise.

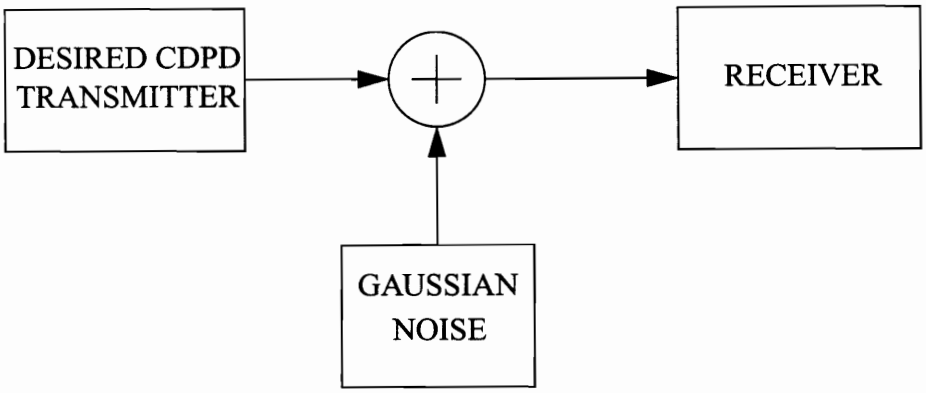

Figure 3-7: Gaussian Noise Model Block Diagram

3.4.2 Rayleigh Fading

The SPW Rayleigh Flat Fading block is used for modeling a flat (or single-ray) Rayleigh fading channel model. The output of this block is the input multiplied by a single complex time-varying weight, known as the "Rayleigh channel weight". This weight is generated by passing complex white Gaussian noise through a fading filter, and then interpolating the output of the fading filter. The fading filter, also known as the spectrum shaping filter, is based on Jakes' model [Jakes74], which has the following frequency response:

$$H(f) = \begin{cases} \dfrac{A}{\sqrt{1-\left(\dfrac{f}{f_d}\right)^2}} & for \quad |f| \le f_d \\ 0 & for \quad |f| > f_d \end{cases} \qquad (3 - 10)$$

In this equation, f_d is the Doppler frequency. Because the Doppler frequency is

usually much less than the sampling frequency, the fading filter response, $H(f)$, is usually a very narrow lowpass filter. To minimize the computational load, the output of the fading filter is interpolated using a Hamming windowed sinc function. The interpolation uses a polyphase filter, so that each iteration requires relatively few multiplies and adds [SPW94]. A block diagram of the model is shown in Figure 3-8.

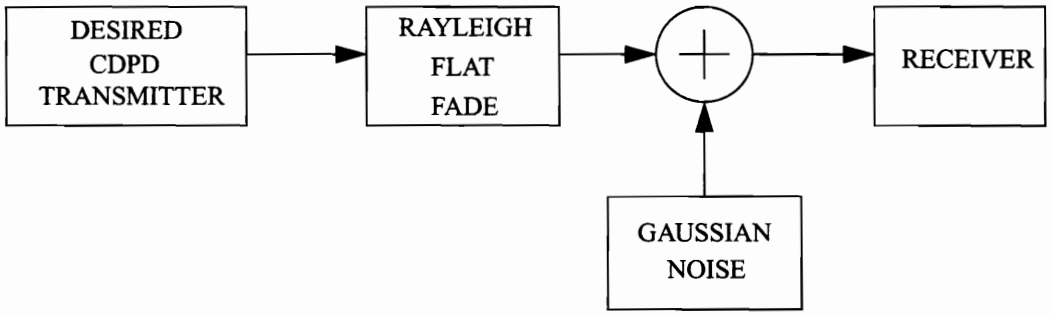

Figure 3-8: Rayleigh Flat Fading Model Block Diagram

The Doppler frequency can be set in the Rayleigh Fading block and simulations were run for the vehicle speeds of 100, 50, and 8 km/hr with Doppler frequencies of 77.408, 38.704, and 6.193 Hz respectively.

3.4.3 Co-Channel Interference

Various co-channel interference simulations were performed the first of which is a CDPD interferer. The block diagram of the model is shown in Figure 3- 9. Multiple simulations were run varying the E_b/N_o, generating a family of curves in which the carrier to interference (C/I) ratio was varied during each simulation. Another set of simulations were run in the same manner using an AMPS interferer instead. An AMPS data file also sampled at 96 kHz was imported into SPW and linked to a signal source block. It's output power could then be controlled to vary the C/I ratio. AMPS co-channel interference simu-

lations are important because they represent the majority of the interfering signals a CDPD signal

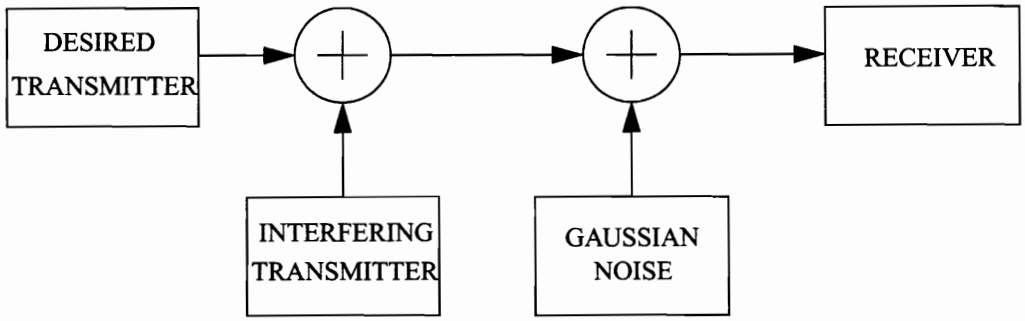

Figure 3-9: Co-channel Interference Model

will encounter. Another AMPS co-channel simulation was run with the desired CDPD transmitter passing through a fading channel. The block diagram of this model is shown in Figure 3-10 below.

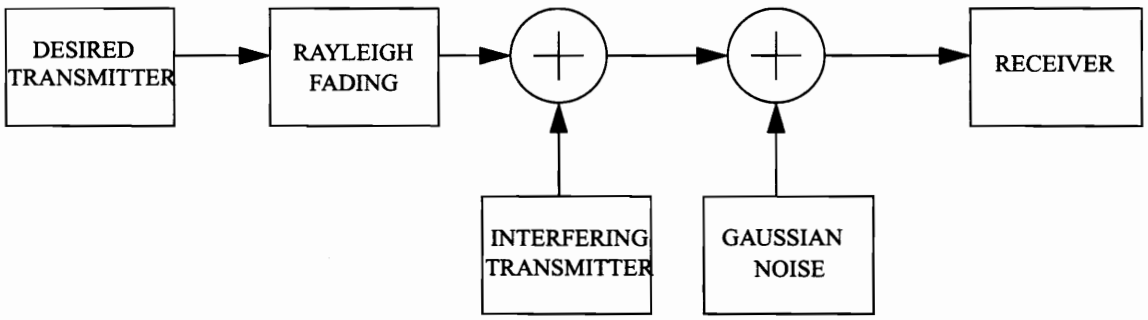

Figure 3-10: Fading Co-channel Interference Model

A final round of simulations were run with a co-channel interference and multipath model. This can be thought of as a two-ray multipath model with a co-channel interferer. The desired signal is first delayed 10 microseconds and then both the desired and time

delayed version of the signal are passed through Rayleigh fading channels. A co-channel interferer is also passed through a fading channel and all are combined and sent to the receiver. Simulations were run for vehicle speeds corresponding to 8 km/hr and 80 km/hr while varying the C/I ratio. The block diagram of this model is shown in Figure 3-11. The results of these simulations will be presented in the following chapter and discussed in Chapter 5.

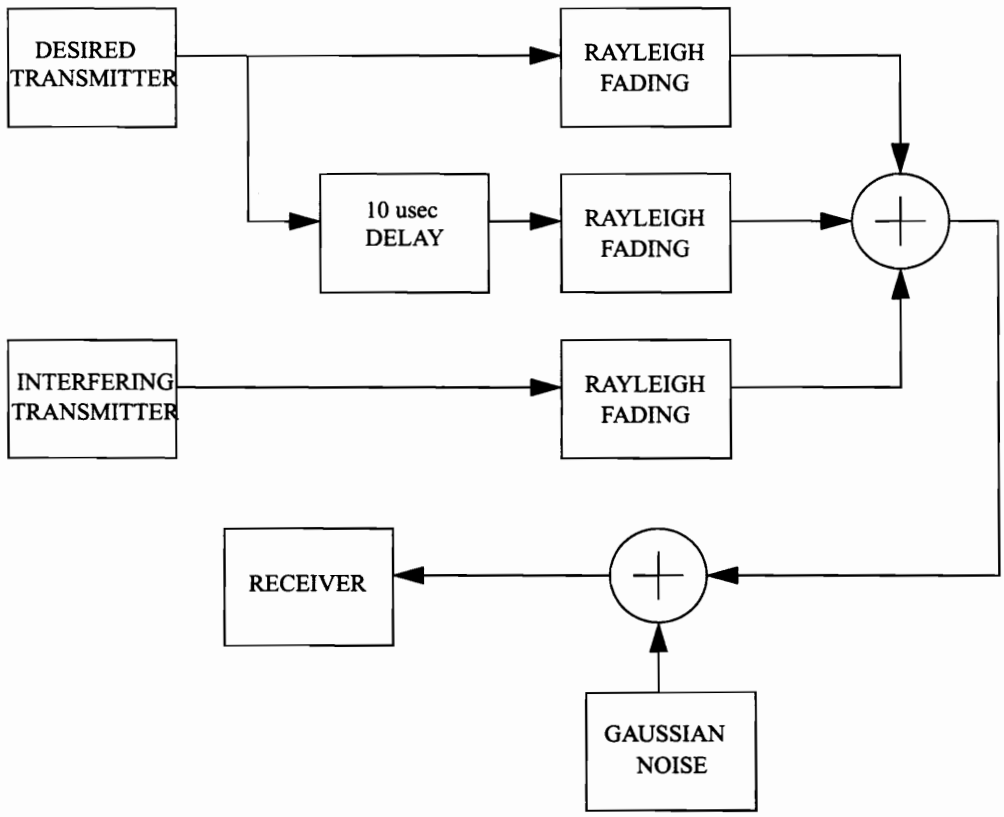

Figure 3-11: Co-channel Interference Rejection and Multipath Model

Chapter 4

Simulation Results

Results from SPW were taken into MATLAB for plotting Bit Error Rate (BER) and Block Error Rate (BLER) curves. The plots for each case follow and are grouped according to the type of simulation.

4.1 AWGN

4.1.1 Differential Detection

Figure 4-1 shows the BER for a Differential Detector in Gaussian Noise. The corresponding BLER graph is shown in Figure 4-2. This model simulates close to ideal channel conditions with noise possibly being introduced at the receiver terminals. The Eb/No is varied for the cases of no coding and Reed-Solomon coding correcting seven symbol errors. The 5% BLER requirement is met at an Eb/No of about 7.8 dB which corresponds to a coded BER of $2*10^{-4}$ and an uncoded BER of $2*10^{-2}$. These bit error rates are quite high, when a BER on the order of 10^{-6} is more desirable. From the above graphs, a BER of 10^{-6} would require a BLER of less than 1%. The gains due to Reed-Solomon encoding can be clearly seen showing a gain of 5 dB in BER and BLER at the 5% tolerance.

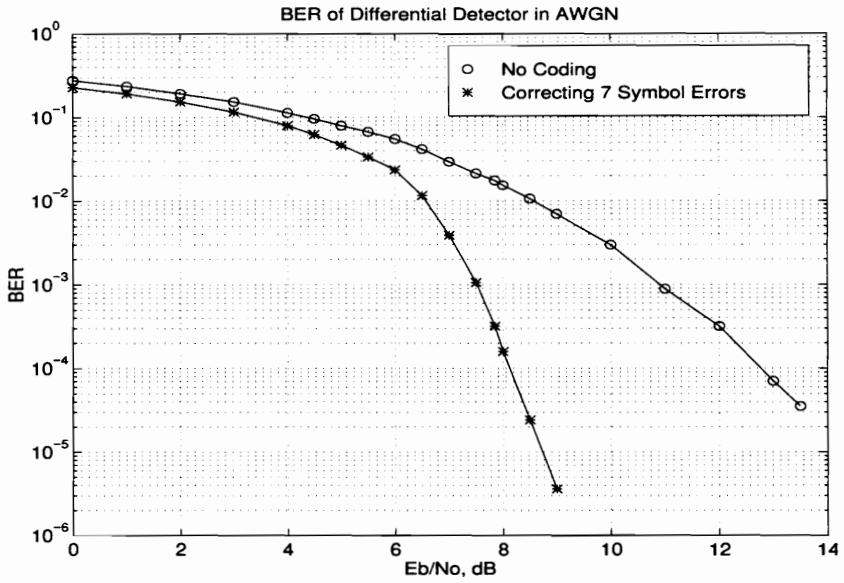

Figure 4-1: BER of Differential Detection in AWGN

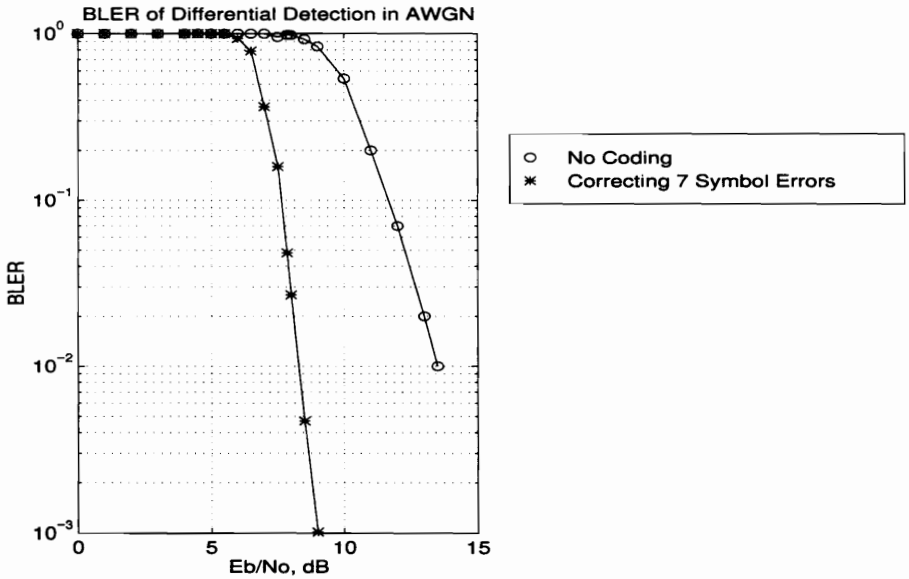

Figure 4-2: BLER of Differential Detection in AWGN

4.1.2 Frequency Discrimination

The same simulations were performed using a frequency discriminator at the receiver instead of a one-bit differential detector. Figure 4-3 shows BER curves for the frequency discriminator while Figure 4-4 shows BLER curves. The results were very similar to the differential detector as was expected from [Simon84] and [Korn91]. The 5% BLER occurs at an Eb/No of approximately 7.5 dB, giving a coded BER of 10^{-4} and uncoded BER of 10^{-2}. Like the differential detector, these BERs are less than ideal and require a strict BLER to drive the BER lower. As stated earlier, these models were useful in verifying the simulator against published work, i.e. comparing the uncoded bit rates of GMSK at a BT = 0.5.

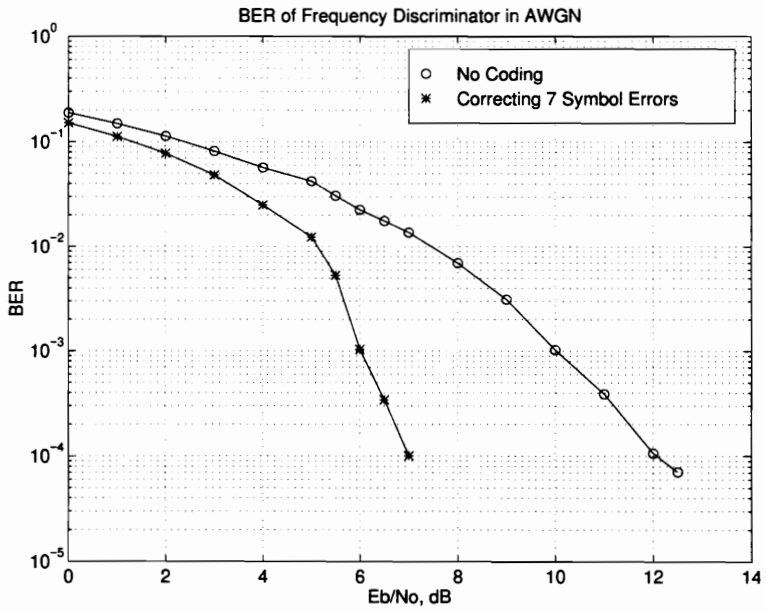

Figure 4-3: BER of Frequency Discriminator in AWGN

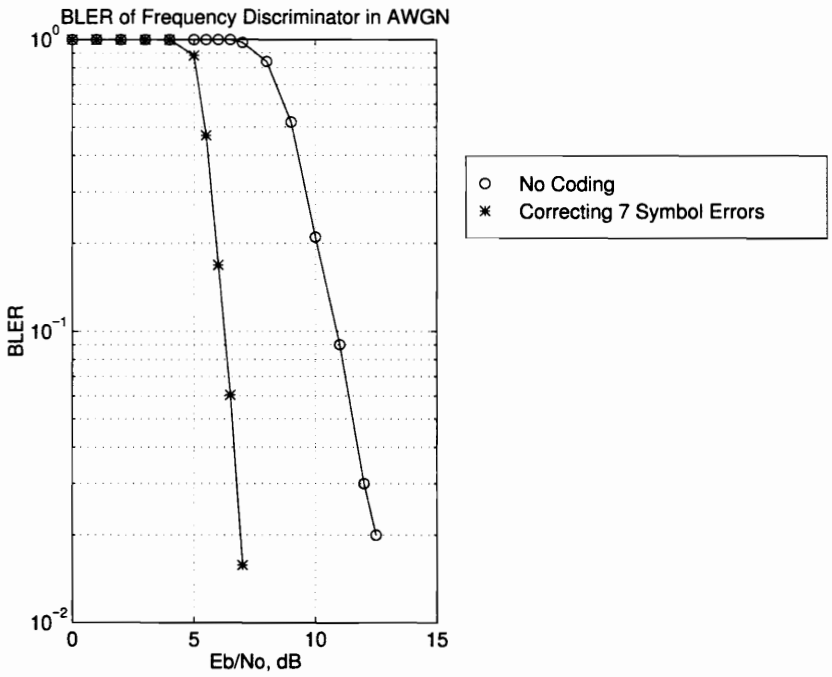

Figure 4-4: BLER of Frequency Discrimination in AWGN

4.2 Rayleigh Fading

Most wireless mobile transmission environments fade with a depth less than 20 dB, with deeper fades in excess of 30 dB being less frequent but not uncommon. A receiver moving at 50 km/hr can pass through several fades a second, or more seriously, it is possible for a vehicle to stop with the antenna in a fade [Pars93]. The CDPD system specification gives performance standards for vehicles moving at 100, 50, and 8 km/hr in flat Rayleigh fading conditions implying that all frequency components are affected in a similar way with no frequency selective behavior. The different vehicle speeds will change the associated Doppler frequency which produces an apparent change of the transmission frequency.

4.2.1 Differential Detection

BER curves for a vehicle traveling at 100 km/hr are shown in Figure 4-5 while BLER curves are shown in Figure 4-6. It is easy to see the more destructive qualities of fading over simple Gaussian noise. The 5% BLER in this case is met at an Eb/No of 18 dB, a much stronger Eb/No than was needed for the noise case. The corresponding BERs remain on the order of 10^{-4} for the coded BER and 10^{-2} for the uncoded.

It is in the fading cases where we begin to see the importance of the Reed-Solomon encoding to the system. Fades tend to cause burst errors in the data stream which the Reed-Solomon code is designed to correct. Correcting up to seven symbol errors (six bit symbols), the (63,47) RS code can overcome some of the effects of fading by correcting portions of the transmission destroyed by the fade. The performance of the Reed-Solomon code also depends on the speed of the vehicle which we will see in the other simulations.

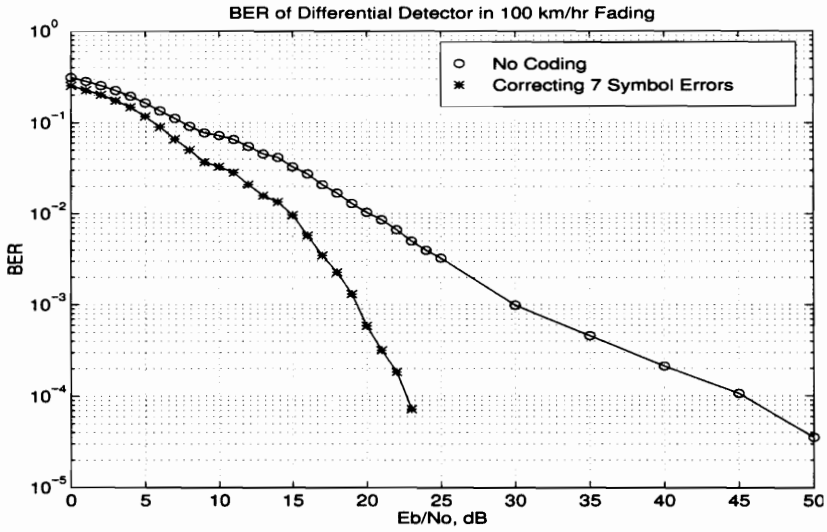

Figure 4-5: BER of Differential Detector in 100 km/hr Fading

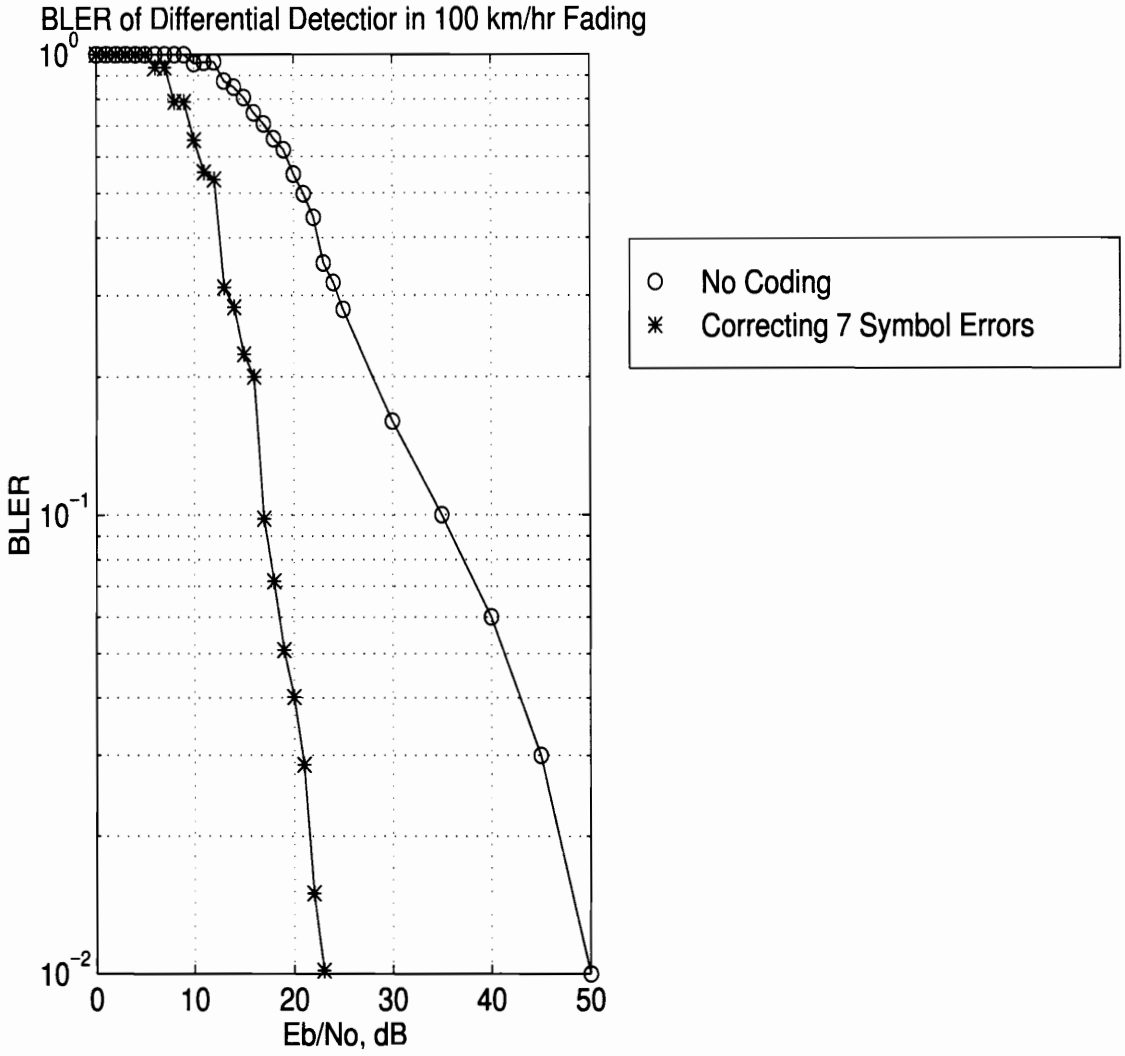

Figure 4-6: BLER of Differential Detector in 100km/hr Fading

Figure 4-7 gives BER curves for a fading simulation with a vehicle speed of 50 km/hr, while Figure 4-8 shows the BLER curves. The Eb/No required for the 5% BLER has moved up slightly to 20 dB implying more signal strength is required in the 50 km/hr case. The corresponding BERs, coded and uncoded, seem to get slightly worse but remain relatively unchanged from the 100 km/hr case.

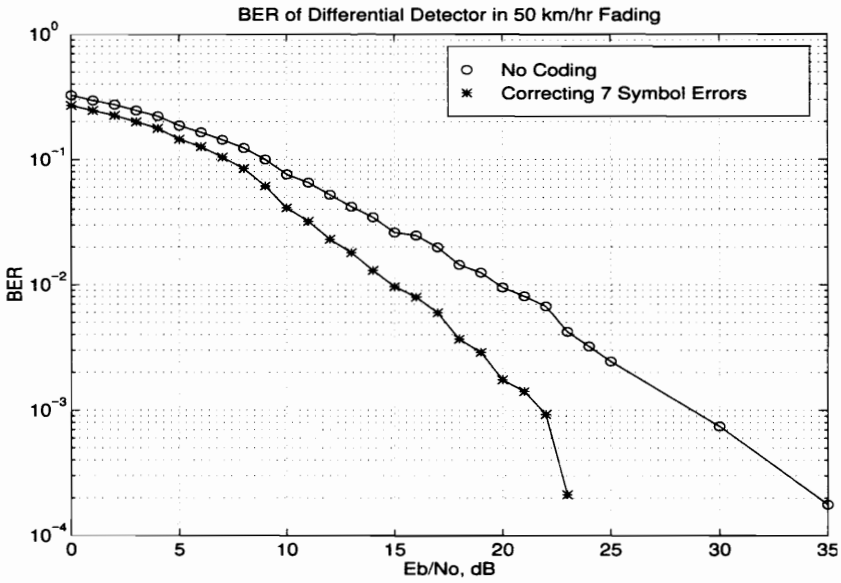

Figure 4-7: BER of Differential Detector in 50 km/hr Fading

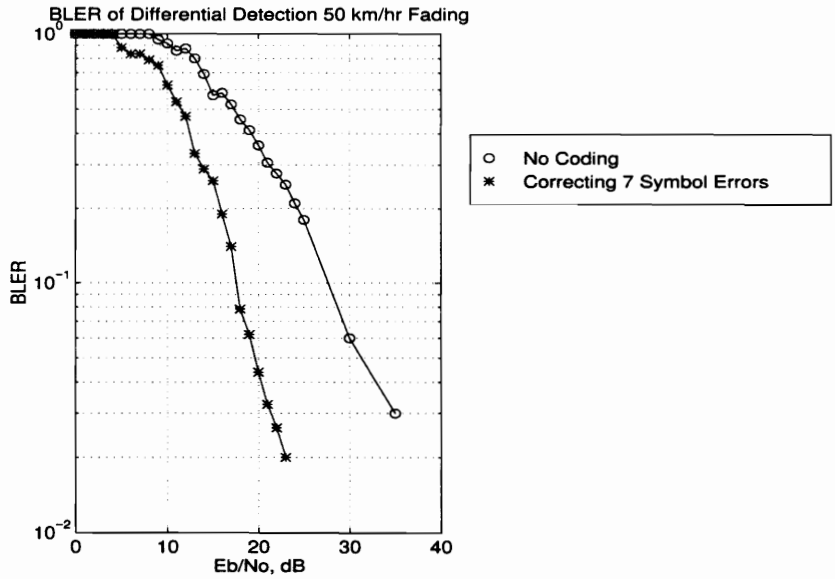

Figure 4-8: BLER of Differential Detector in 50 km/hr Fading

The final fading simulation was run at a vehicle speed of 8 km/hr and the results are shown in Figures 4-9 and 4-10. In this case the 5% BLER was achieved at an Eb/No of 23 dB, the highest Eb/No needed of the fading cases. Again the BERs remain on the same order of magnitude as in previous cases with only slight variations. These results show a trend of poorer performance at slower vehicle speeds which is a significant outcome. The fades last longer defeating the advantages of RS encoding. Interleaving would have been a beneficial addition to the standard for low speed applications.

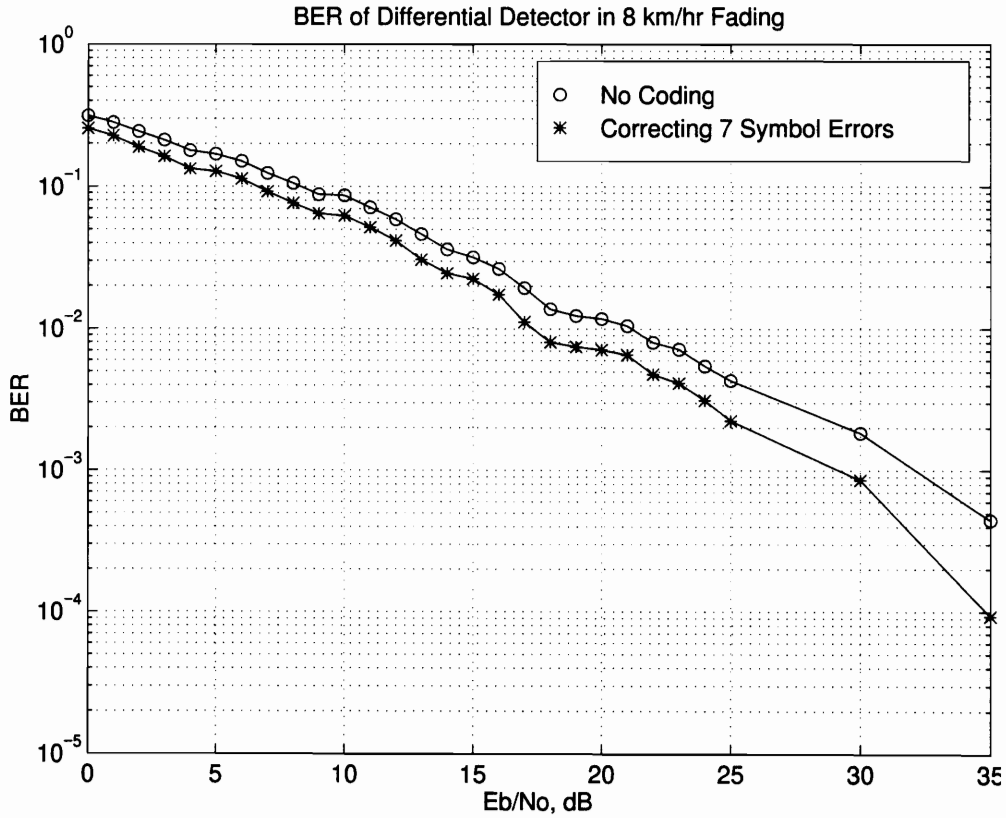

Figure 4-9: BER of Differential Detector in 8 km/hr Fading

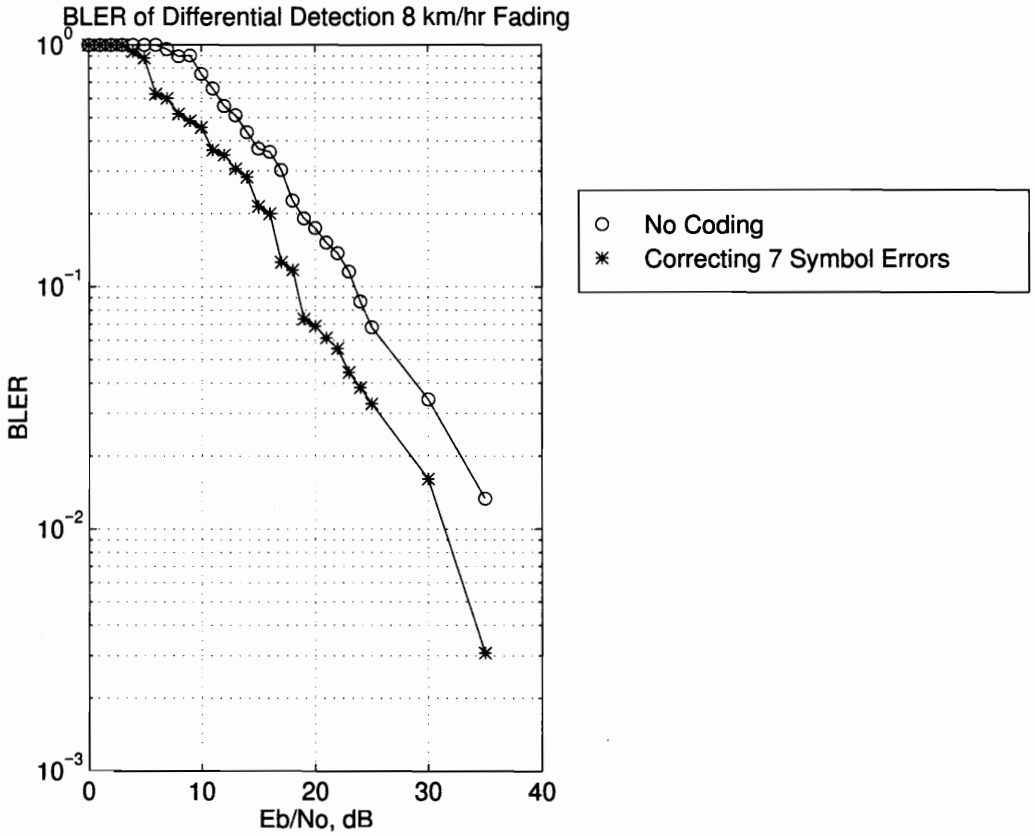

Figure 4-10: BLER of Differential Detector in 8 km/hr Fading

4.2.2 Frequency Discrimination

The same fading simulations were run using a frequency discriminator instead of the differential detector. Figures 4-11 and 4-12 show the results for the 100 km/hr fading case. When compared to the differential detector, the BLER performance is practically identical while the corresponding BERs at the 5% BLER are slightly better for the frequency discriminator, but very close.

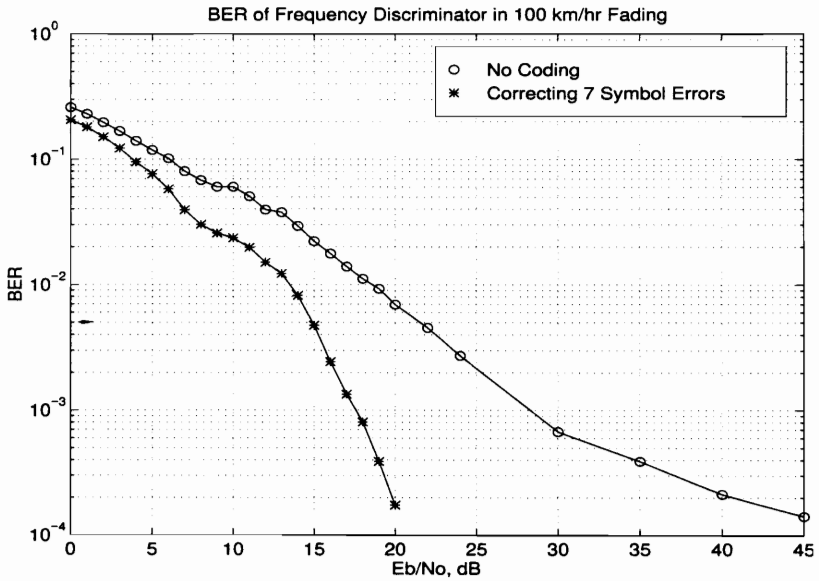

Figure 4-11: BER of Frequency Discriminator in 100 km/hr Fading

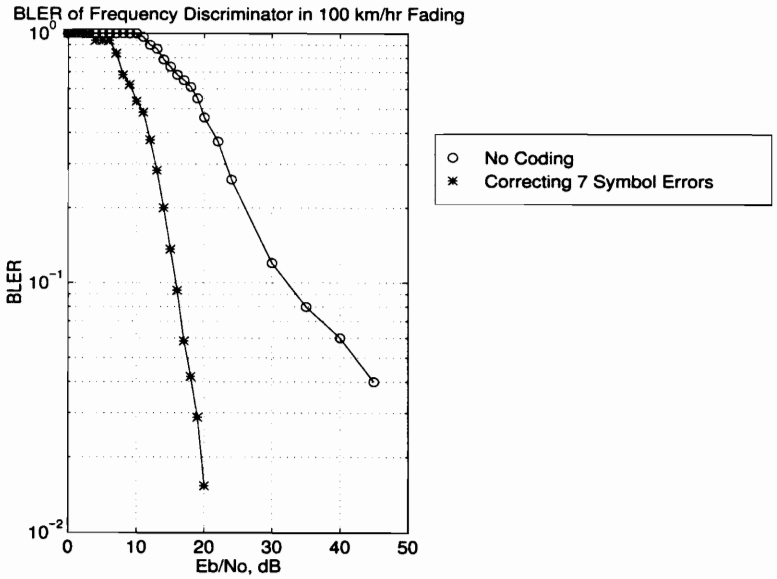

Figure 4-12: BLER of Frequency Discriminator in 100 km/hr Fading

The BER and BLER curves for the frequency discriminator in 50 km/hr fading are shown in Figure 4-13 and 4-14. Again, the results are nearly identical as for the differential detector with the 5% BLER occurring at an Eb/No of 19 dB. As well as in the differential detection case, we still see the trend of poorer performance at the slower vehicle speeds. Coding gains from the Reed-Solomon codes also become less significant at the slower vehicle speeds implying that the correction capabilities of the Reed-Solomon code are being exceeded at the lower speeds.

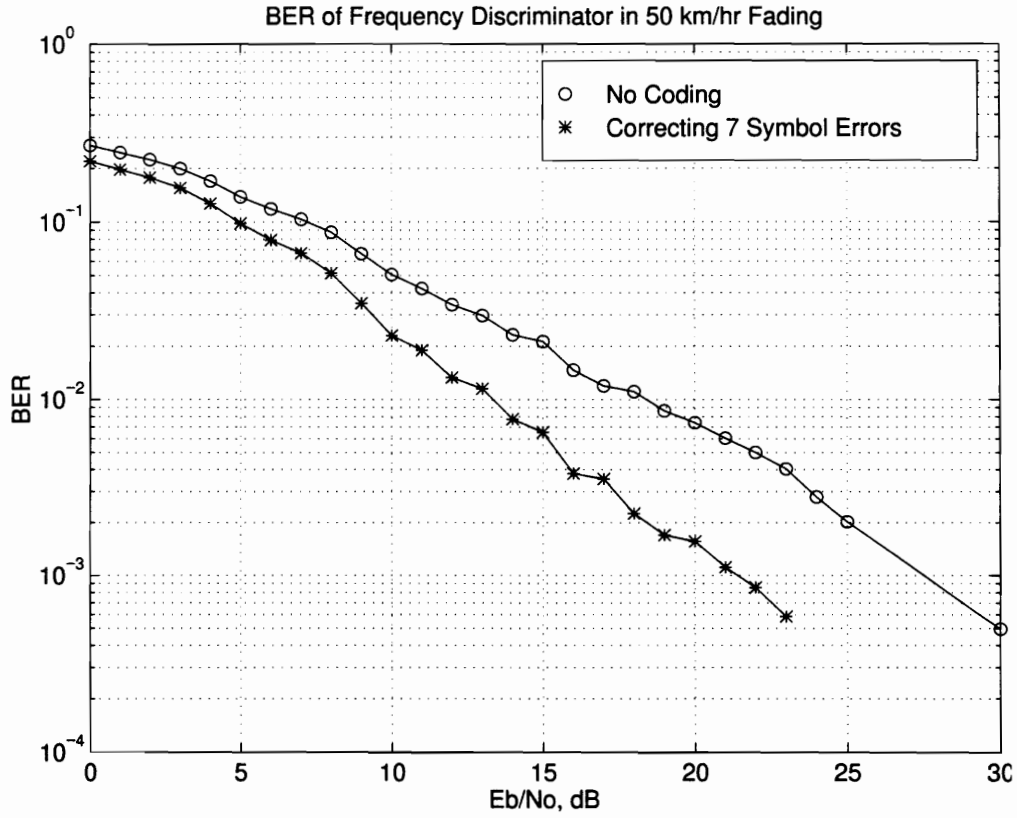

Figure 4-13: BER of Frequency Discriminator in 50 km/hr Fading

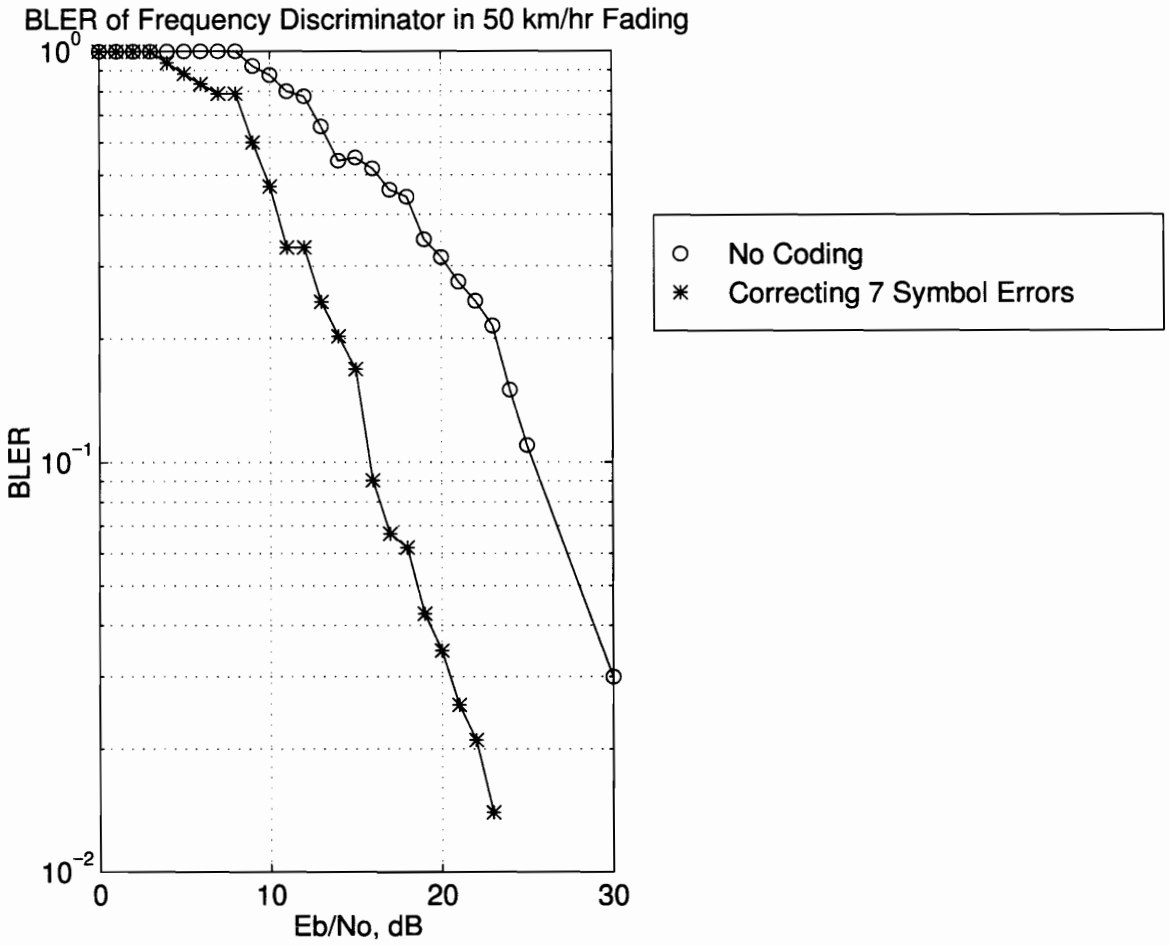

Figure 4-14: BLER of Frequency Discriminator in 50 km/hr Fading

The 8 km/hr fading cases are shown in Figures 4-15 and 4-16. As with the differential detector, this fading case produces the poorest conditions of all requiring an Eb/No of 22 dB to accommodate the 5% BLER. The coding gain in this case, about 4 dB at the 5% BLER, is very minimal as compared to the other fading cases.

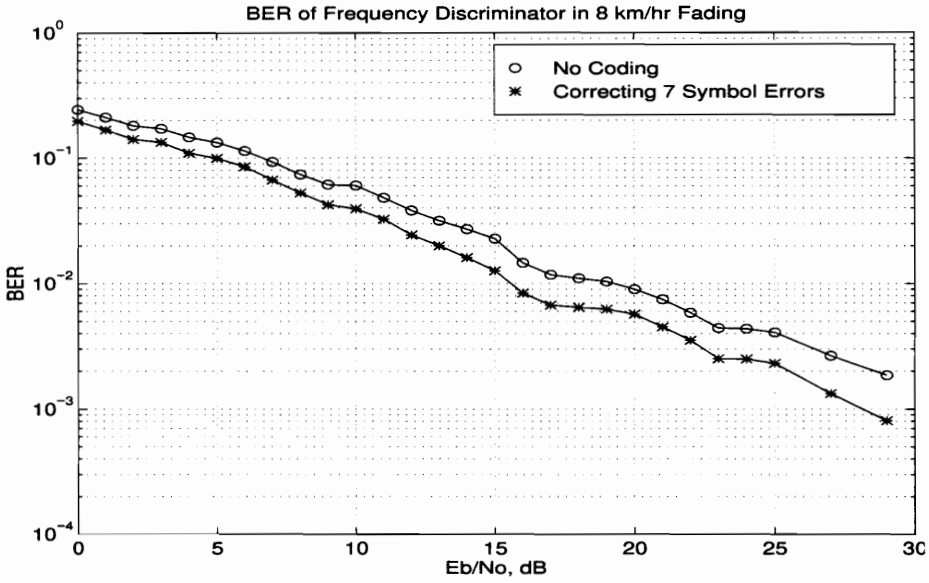

Figure 4-15: BER of Frequency Discriminator in 8 km/hr Fading

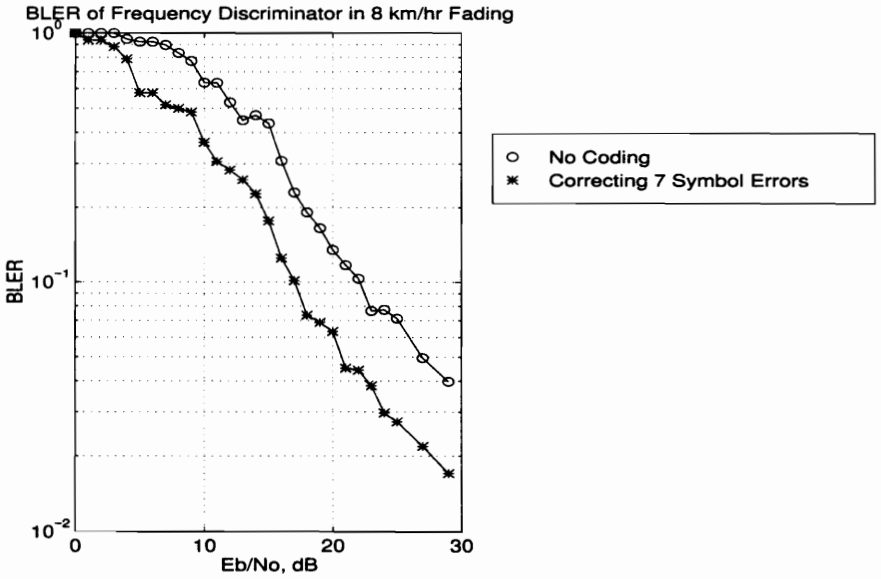

Figure 4-16: BLER in 8 km/hr Fading

4.3 Co-Channel Interference

4.3.1 CDPD

A series of co-channel interference simulations were also run beginning with CDPD interference. This simulation involved setting the Eb/No at a given value and varying the carrier to interference (C/I) ratio to obtain a family of curves. Simulations were run for Eb/Nos of 7, 8 and 10 dB and the results are shown in Figures 4-17 and 4-18. It is unlikely that the co-channel interferer will be another CDPD signal, yet the possibility still exists. The remaining simulations use the differential detector at the receiver.

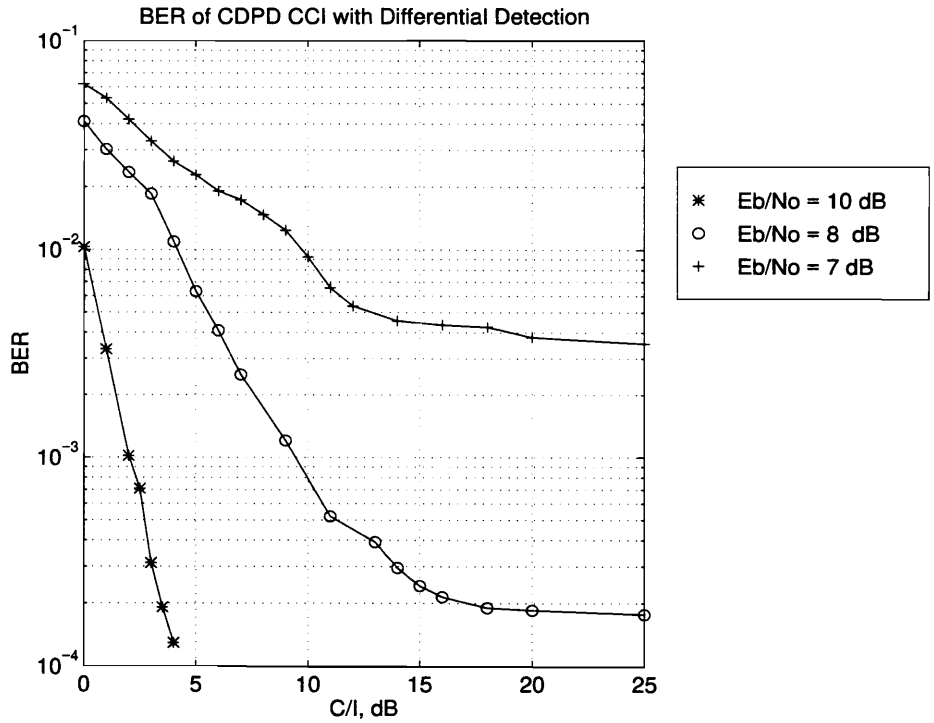

Figure 4-17: BER with CDPD Interferer in Gaussian Noise

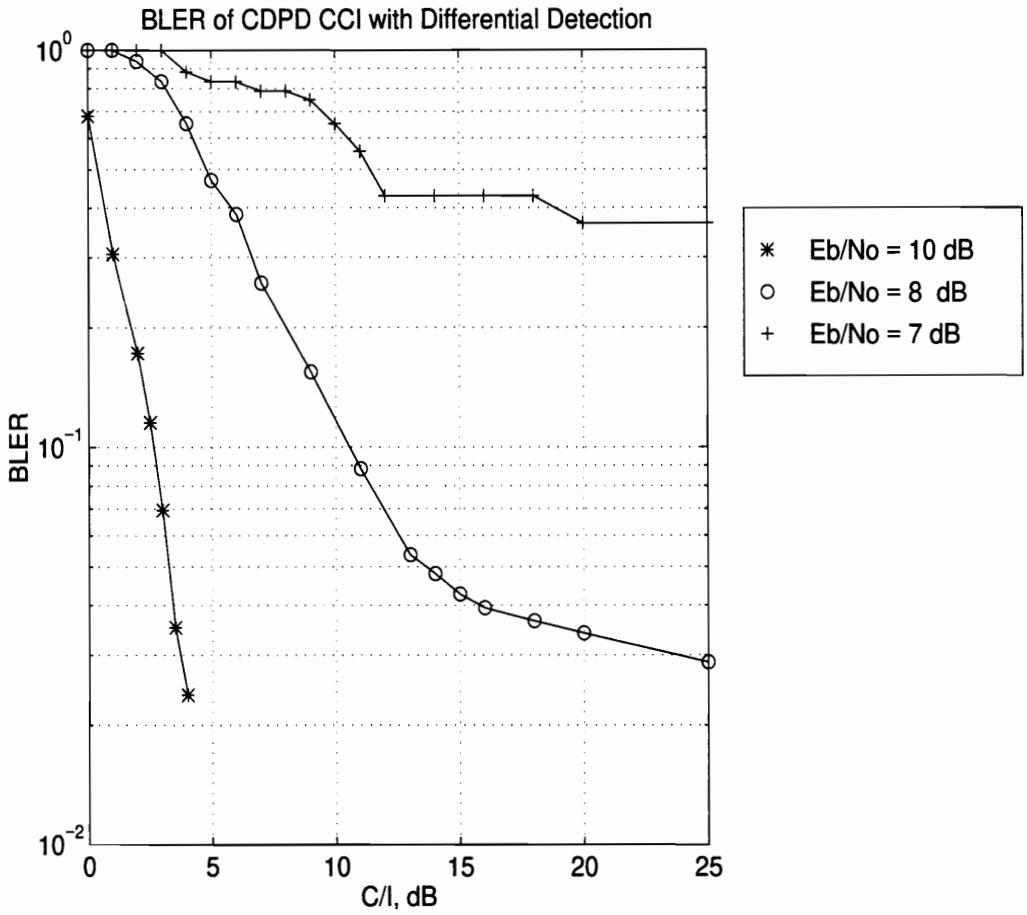

Figure 4-18: BLER with CDPD Interferer in Gaussian Noise

Figure 4-18 shows that an Eb/No of 7 dB could not meet the 5% BLER requirement while an Eb/No of 8 dB did meet the requirement but becomes noise limited at a BLER of about 2%. The 10 dB Eb/No simulation easily met the 5% BLER and is only limited by the amount of interference.

4.3.2 AMPS

AMPS co-channel interference simulations were also run in the same manner for

Eb/Nos of 7, 8 and 10 dB. It is highly likely that a CDPD signal will have an AMPS signal as its interferer in a true cellular environment. Figure 4-19 shows a family of BER curves while Figure 4-20 shows a family of BLER curves for the same Eb/Nos. The results are similar to the CDPD interferer simulations in that the 7 dB Eb/No simulation could not achieve the required 5% BLER, but the 8 and 10 dB simulations did.

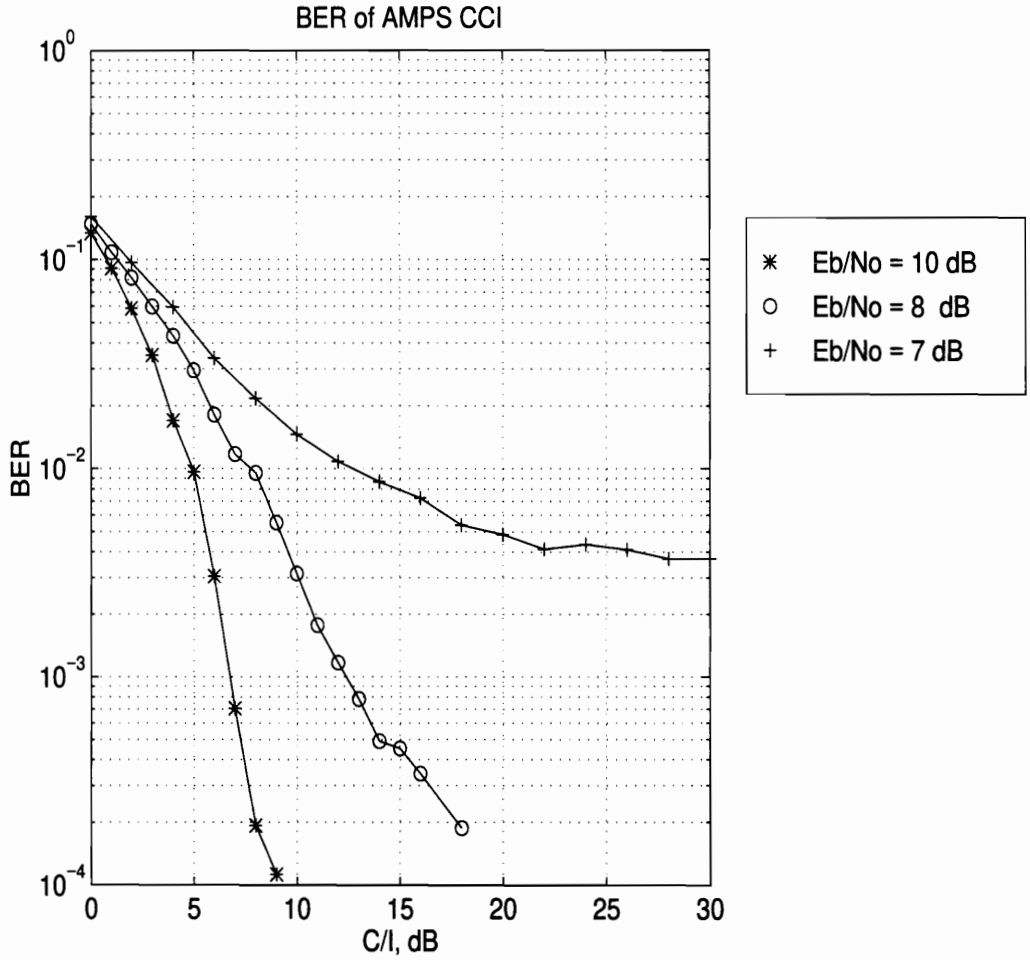

Figure 4-19: BER with AMPS Interferer in Gaussian Noise

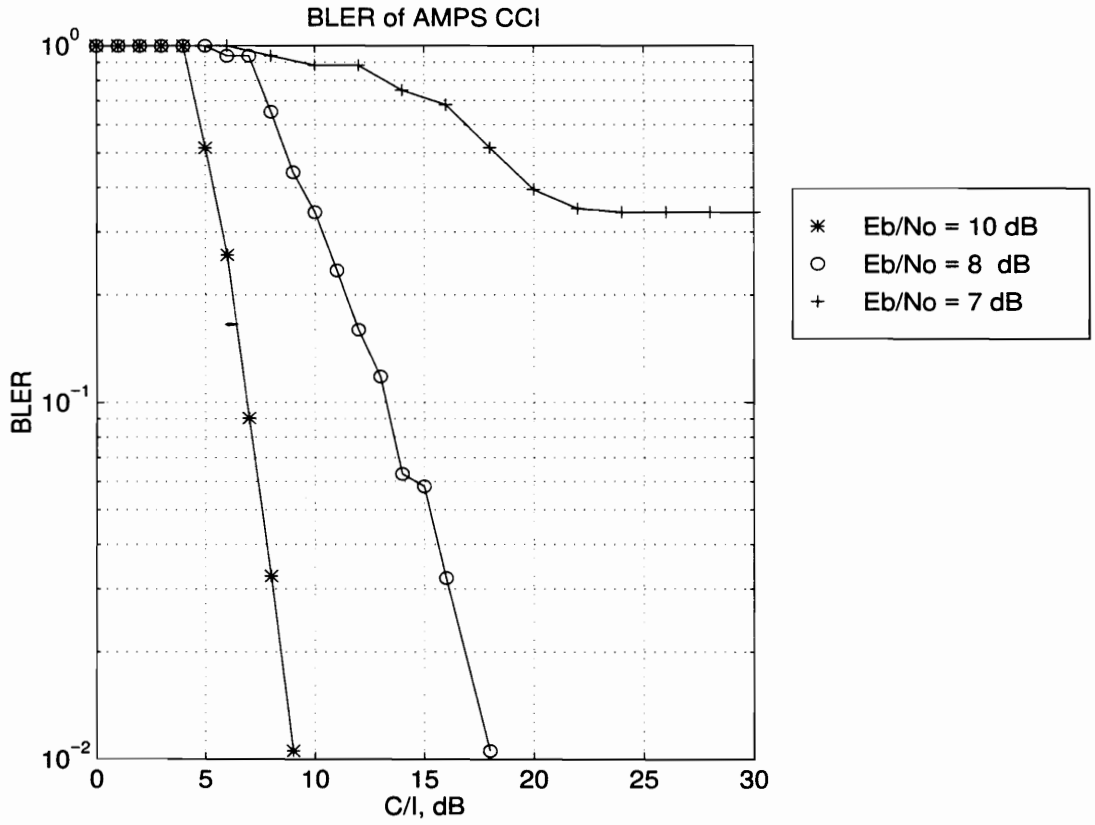

Figure 4-20: BLER with AMPS Interferer in Gaussian Noise

The simulations also show that the AMPS co-channel interference is more destructive to a CDPD signal than CDPD interference. The CDPD interference simulation required a C/I ratio of 13 dB to reach the 5% BLER for an Eb/No of 8 dB where the AMPS interference simulation requires a C/I ratio of 16 dB to reach the 5% BLER for the same Eb/No. This is a significant result since a CDPD signal will encounter AMPS interferers a majority of the time. This also gives insight to cell planning and setting aside select AMPS channels for CDPD.

A further AMPS co-channel interference simulation was run, this time with the desired CDPD signal being faded. This simulation realizes a more typical mobile environ-

ment where fading is the dominant mechanism and interference is also present. For this simulation the Eb/No was set at 30 dB and the C/I ratio was varied. Figure 4-21 shows the resulting BER curve while Figure 4-22 presents the BLER curve. The 5% BLER tolerance is met at an C/I of 16 dB, but it must be remembered that this is at an Eb/No of 30 dB, much higher than the co-channel interference simulations with no fading where the 5% BLER was also met at a C/I of 16 dB, but with an Eb/No of 8 dB.

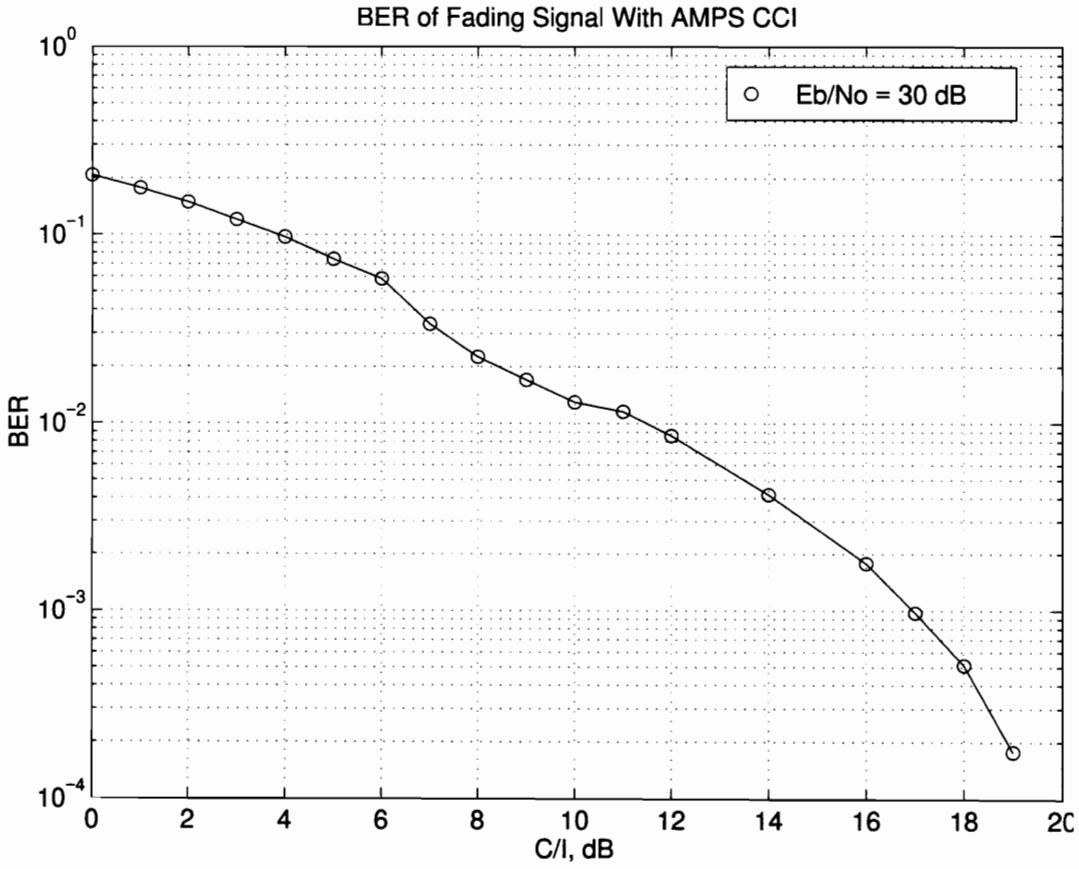

Figure 4-21: BER of Fading CDPD Signal with AMPS Interference

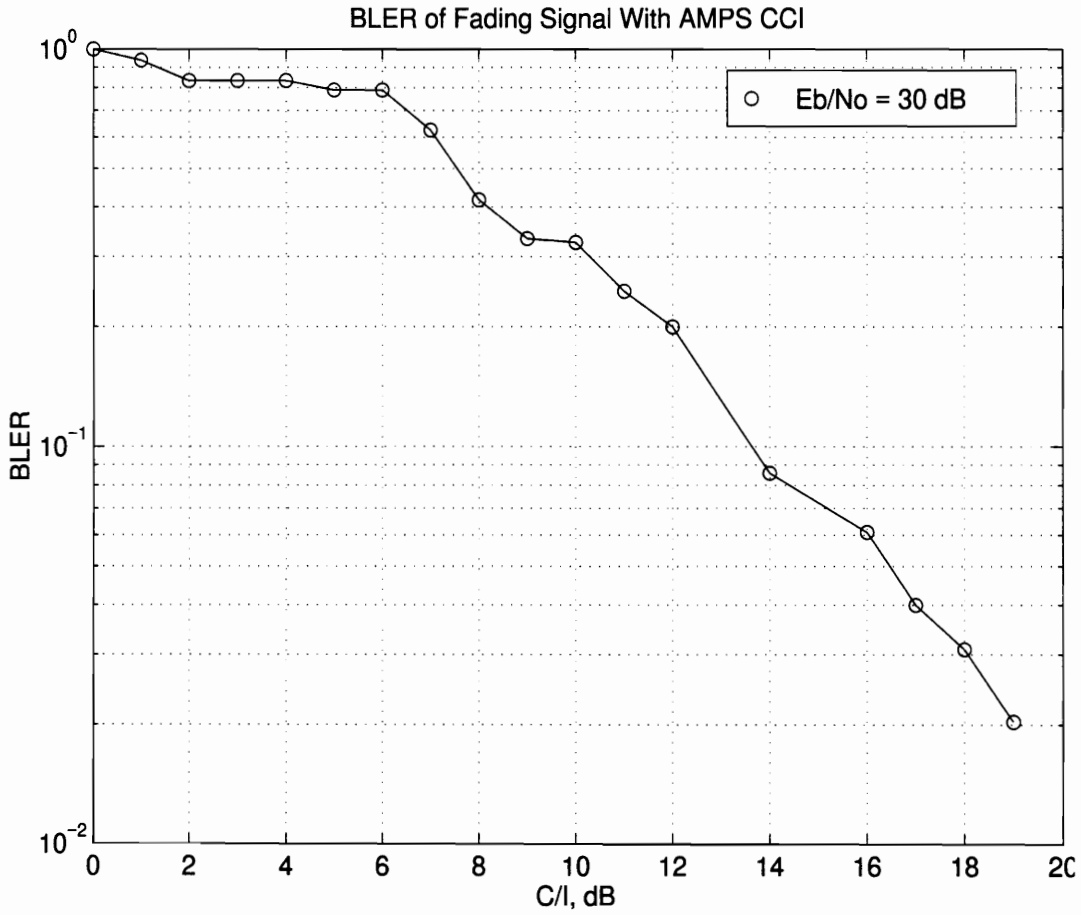

Figure 4-22: BLER of Fading CDPD Signal with AMPS Interference

A final round of simulations were run according to the CDPD System Specification involving a multipath and co-channel interference model. A desired signal is delayed 10 uS and both the delayed and original versions of the signal are passed through Rayleigh fading models. A faded co-channel interferer is also introduced as well as Gaussian noise before being sent to the receiver. Simulations were run at 8 and 80 km/hr according to the specification.

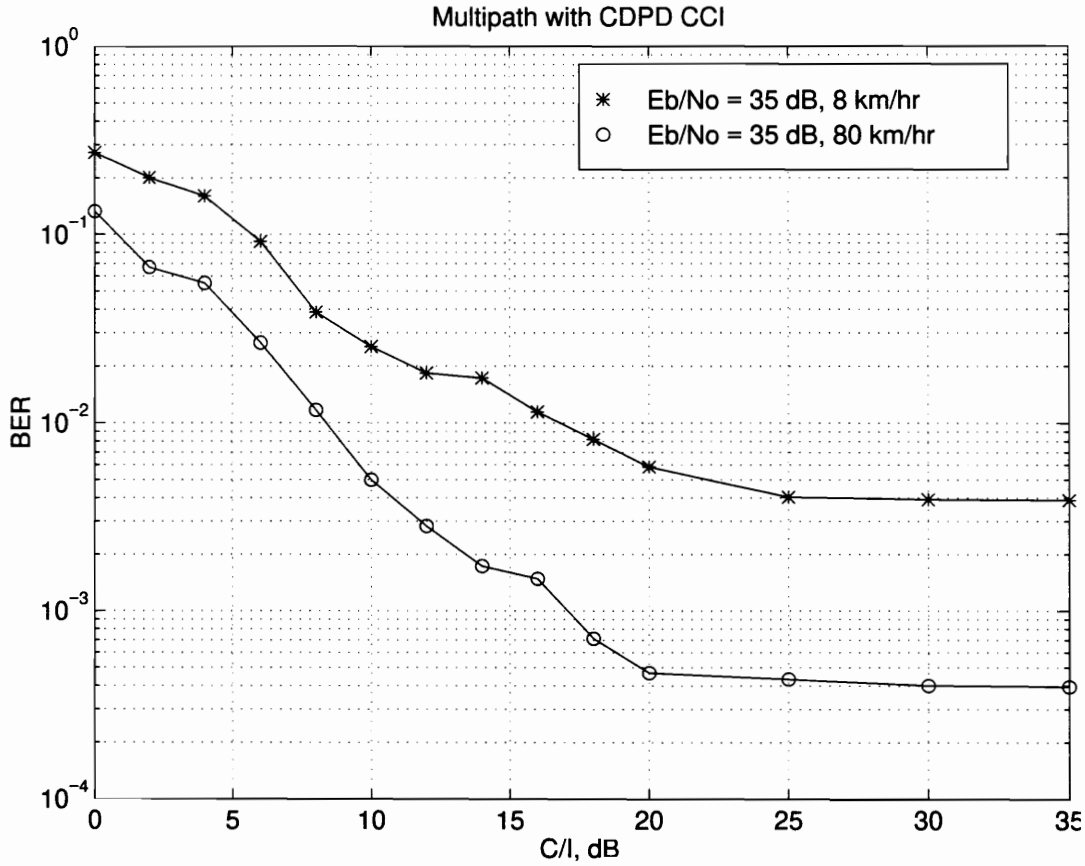

Figure 4-23: BER of Multipath Model with CCI at 8 and 80 km/hr

Figure 4-23 shows the BER curves for both the 8 and 80 km/hr cases while Figure 4-24 shows the BLER curves. Both the 8 and 80 km/hr simulations were run with an Eb/No of 35 dB while varying the C/I.

Again there is a trend for poorer performance at slower vehicle speeds as was found in the earlier fading cases. The 8 km/hr simulation reaches 5% BLER at 25 dB of C/I while the 80 km/hr simulation reaches the same requirement at 17 dB of C/I. Both simulations become noise limited as the C/I grows, the 8 km/hr simulation levels off at a 4% BLER and the 80 km/hr simulation at a 2% BLER. A stronger Eb/No may lower this noise

threshold which would be needed to reach lower BERs than those on the order of 10^{-3}.

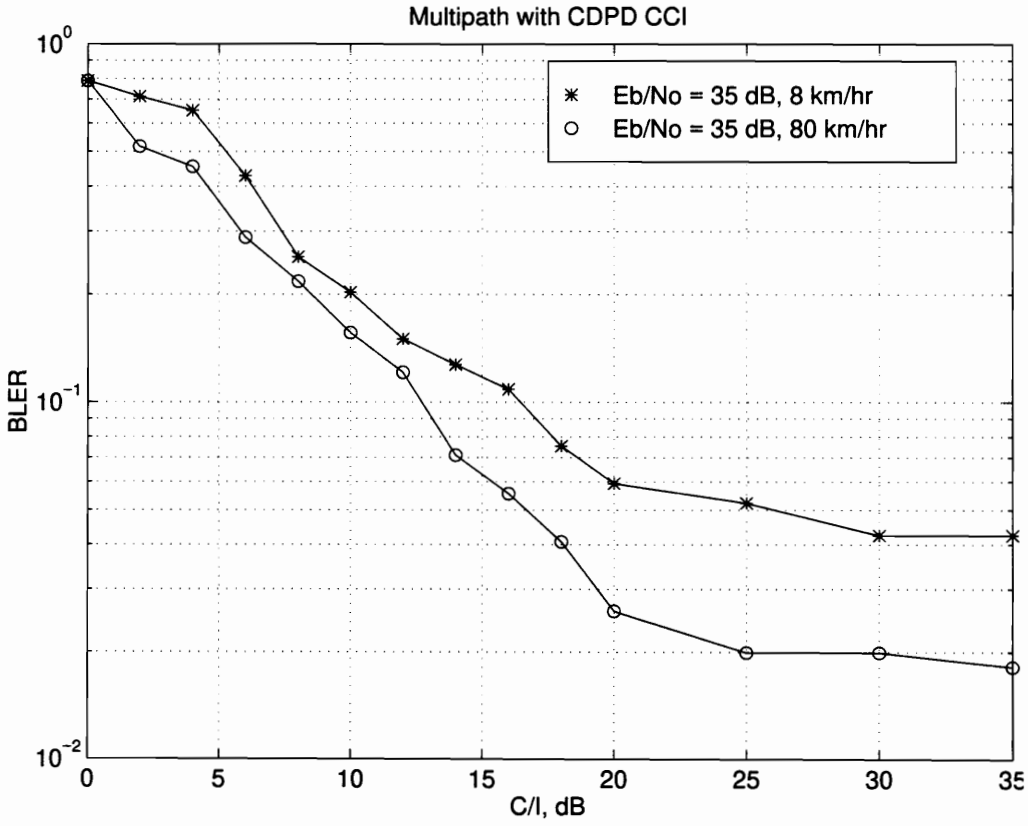

Figure 4-24: BLER of Multipath Model with CCI at 8 and 80 km/hr

Chapter 5

Conclusions

5.1 Summary of The Research

Table 5-1 shows the point at which a 5% Block Error Rate was reached for the Gaussian Noise and Rayleigh Fading cases. The first three entries correspond to the Frequency Discriminator while the last three are for the Differential Detector. Block Error Rate coding gains are also calculated as are the corresponding Bit Error Rates that occur at the coded 5% BLER value.

The CDPD specification allows 5 bit errors out of 35 in the forward channel synchronization word and 3 bit errors out of 22 in the reverse channel synchronization word, both of which are not Reed-Solomon encoded. This roughly translates to a BER of 1.4 $*10^{-1}$ in both cases for the uncoded data. The above results seem to satisfy this requirement for an uncoded BER, but still leave the operating conditions at a relatively undesirable level for both coded and uncoded BERs. The coded BERs tend to be on the order of 10^{-3} for every simulation at the 5% BLER, where a lower BER of 10^{-6} would be more desirable.

With the fading cases, the coded BLER tends to be worse at slower vehicle speeds than at higher vehicle speeds. A slower vehicle will spend more time in a fade relative to the length of a Reed-Solomon block than a faster vehicle. The number of symbols per block in error will increase for the slower vehicle for this reason and more undecodeable Reed-Solomon blocks will result. A higher signal strength is needed to compensate for the

fading.

Table 5-1: Eb/No and Bit Error Rates at 5% BLER

[redacted]	Eb/No To Achieve 5% BLER (dB)			Corresponding Bit Error Rate		
	Coded	Uncoded	Gain	Coded	Uncoded	Receiver
AWGN	7.5	12	4.5	10^{-4}	10^{-2}	Freq. Dis.
100 km/ hr fading	18	43	25	$3*10^{-4}$	$9*10^{-3}$	Freq. Dis.
50 km/hr fading	19	29	10	$1.8*10^{-3}$	$8*10^{-3}$	Freq. Dis.
8 km/hr fading	21.5	27	5.5	$5*10^{-3}$	$7*10^{-3}$	Freq. Dis.
AWGN	7.8	12.5	4.7	$2*10^{-4}$	$2*10^{-2}$	Diff. Det.
100 km/ hr fading	18	42	24	$8*10^{-4}$	$1.5*10^{-2}$	Diff. Det.
50 km/hr fading	19.5	32	13	$1*10^{-3}$	$1*10^{-2}$	Diff. Det.
8 km/hr fading	23	27	4	$2*10^{-3}$	$7*10^{-3}$	Diff. Det.

A comparison in receivers shows that the frequency discriminator and the differential detector perform approximately the same under all conditions with the slight edge going to the frequency discriminator (in terms of BLER). A more complex differential detection scheme would probably show the opposite to be true. Two- and three-bit differential detection with and without feedback as well as combined differential detection schemes are likely to outperform a frequency discriminator.

CDPD co-channel interference simulations were run in Gaussian noise to generate a family of curves for bit and block error rates with Eb/Nos of 7, 8 and 10 dB. While the 7

dB signal strength simulation did not meet the 5% BLER, the 8 dB simulation met the requirement with a C/I of about 13 dB. At this Eb/No the system still seems to become noise limited at a BLER of 2.5%. An Eb/No of 10 dB clearly achieved the required tolerance with ease limited only by the level of interference. The BER of the 8 dB signal is still on the order of 10^{-3} which leaves room for improvement.

AMPS co-channel interference simulations show the same trends with an Eb/No of 8 dB achieving the desired 5% BLER but at a higher C/I ratio than the CDPD interferer. This demonstrates that an AMPS interferer could prove to be more destructive to a CDPD signal than another CDPD interferer. This is a very telling statistic since a CDPD signal will more than likely see interference from an AMPS user than another CDPD user. This result could prove helpful in frequency planning.

A more realistic simulation, therefore, is the fading CDPD signal with an AMPS interferer. The simulations were run with an Eb/No of 30 dB while varying the C/I ratio with a 5% BLER occurring at about 16 dB of C/I. Fading proves to be a dominant mechanism in these simulations requiring a much larger Eb/No to overcome the effects. Even at this Eb/No, the corresponding BER is barely 10^{-3}, still too high for many applications.

A final round of simulations included a multipath component with a delay of 10 uS as well as a co-channel interferer and Gaussian noise with fading applied to all signals. Simulations were run for vehicle speeds of 8 and 80 km/hr. These simulations show the same trend as the earlier fading simulations in that poorer performance occurs at slower vehicle speeds and fading is the dominant channel impairment. A 10 uS delayed multipath component would seem to give rise to constructive interference since a single bit time is about 52 uS. Independent fading characteristics imposed on each signal path change the constructive/destructive properties of the interference. Even at an Eb/No of 35 dB, these simulations perform roughly equally as the fading/co-channel interference simulations

with no multipath.

Rayleigh fading is a primary cause of burst errors over the CDPD airlink. This is a good reason for the use of Reed-Solomon codes which use error correction on symbols rather than bits. Still, at slower vehicle speeds, fading can become severe enough to overcome the correction capabilities of the code. One solution might be to increase the number of bits per symbol in the code, but this tends to increase the size of the Reed-Solomon code itself. CDPD's packet-switched and frequency hopping nature would not be suitable for longer Reed-Solomon codes. Another solution my be the use of interleaving as well as Reed-Solomon encoding to eliminate the burst errors caused by fading. This is a fairly simple and proven technique employed by other systems such as Code Division Multiple Access (CDMA).

5.2 Future Work

Once a widespread CDPD roll out begins, there will certainly be a need for deeper research into capacity and throughput issues, especially in large urban areas where idle times on existing cellular networks are becoming less frequent. CDPD's possible use in Intelligent Vehicle Highway System (IVHS) applications would also put greater demands on its use from a capacity standpoint. Other software packages would better lend themselves to this type of modeling and research than SPW because of the limited large scale network modeling capabilities of SPW.

Research into receiver implementations for the detection of GMSK is always a continuing effort and, as mentioned before, more complex differential detection schemes have resulted because of this work. Decoding algorithms for Reed-Solomon codes, such as the use of erasure decoding, is another area where continuing research may be useful.

References

[Abra93] Abrardo, A., A. Abrardo, G. Benelli and G. Cau, "Multiple symbols differential detection of GMSK", IEE 1993., G. Benelli and G. Cau, "Multiple symbols differential detection of GMSK", IEE 1993.

[AHA95] Advanced Hardware Architectures, *Reed-Solomon Error Correction Codes(ECC)*, Advanced Hardware Architectures, Pullman, WA 1995.

[ARDIS95] ARDIS Web Page, http://www.ardis.com, 1995 ARDIS.

[Berl87] Berlekamp, E., R. Peile, and S. Pope, The Application Of Error Control to Communications", IEEE Communications Magazine, Vol. 25, No. 4, pp. 44-57, April 1987.

[CDPDW95] CDPD Forum Web Page, http://www.cdpd.org, 1995 CDPD Forum.

[CDPDS95] *Cellular Digital Packet Data System Specification, Release 1.1*, January 19, 1995.

[Couch93] Couch, Leon W., *Digital And Analog Communication Systems*, Fourth Edition, Macmillan Publishing Company, New York, 1993.

[Elon87] Elnoubi, Said M., "Analysis of GMSK with Two-Bit Differential Detection in Land Mobile Radio Channels", IEEE Transactions on Communications, vol. com-35, no. 2, February 1987.

[Gall94] Gallant, John, "The CDPD Network", EDN, p. 41, October 13, 1994.

[Jacobs94] Jacobsmeyer, Jay M., "Improving Throughput and Availability Of Cellular

Digital Packet Data (CDPD)", Proceedings Of Virginia Tech's Fourth Symposium On Wireless Personal Communications, June 1-3, 1994

[Jacobs95] -----, "Capacity of Channel Hopping Channel Stream On Cellular Digital Packet Data", Proceedings Of Virginia Tech's Fifth Symposium On Wireless Personal Communications, May 31- June 2, 1995.

[Jakes74] Jakes, W.C., *Microwave Mobile Communications*, J. Wiley, 1974.

[Korn91] Korn, Israel, "GMSK with Limiter Discriminator Detection in Satellite Mobile Channel", IEEE Transactions on Communications, vol. 39, no.1, January 1991.

[Lee93] Lee, William C., *Mobile Communication Design Fundamentals*, John Wiley & Sons, New York, 1993

[Lin83] Lin, Shu and D.J. Costello, *Error Control Coding: Fundamentals and Applications*, Prentice Hall, Englewood, N.J., 1983.

[Merrill94] Merrill, Michael, "Waiting For CDPD", Cellular Business, p. 34, February 1994.

[Moeller94] Moeller, Mike, "Carriers Race To Provide CDPD", Cellular Business, p. 43, February 1994.

[Murota81] Murota, K. and K Hirade, "GMSK Modulation For Digital Mobile Telephony", *IEEE Trans. Commun.*, vol. COM-29, pp. 1044-1050, July 1981.

[Pars93] Parsons, David, *The Mobile Radio Propagation Channel*, Halsted Press a Division of John Wiley and Sons, New York, 1993.

[Puk94] Puk, Kevin, *Cellular Digital Packet Data (CDPD): An Overview*, Release 1.0, June 9 1994.

[RAM95] RAM Mobile Data Web Page, http://www.ram-wireless.com, 1995 RAM Mobile Data USA Limited Partnership.

[Reed60] Reed, I. S. and G. Solomon, "Polynomial Codes Over Certain Finite Fields", J. Soc. Ind. Appl. Math., Vol. 8, pp. 300-304, and Math. Rev. Vol. 23B, P. 510, 1960.

[Shib93] Shibata, K., "Error Performance of Two Decision Schemes for Frequency-Detector Gaussian Minimum Shift Keying (GMSK) on a Frequency Selective Fading Channel", Electronics and Communications in Japan, Part 1, vol. 76, no. 2, 1993.

[Shin93] Shin, Soon and P. Mathiopoulos, "Differentially Detected GMSK Signals in CCI Channels for Mobile Cellular Communication Systems", IEEE Transactions on Vehicular Technology, vol. 42, no. 3, August 1993.

[SPW94] Signal Processing Worksystem Users Manuals, Comdisco Systems A Business Unit Of Cadence Design Systems, Inc., 1994.

[Simon83] Simon, M. and C. Wang, "Differential Versus Limiter-Discriminator Detection of Narrow-Band FM", IEEE Transactions On Communications, vol. com-31, no. 11, November 1983.

[Simon84] -----, "Differential Detection of Gaussian MSK in a Mobile Radio Environment", IEEE Transactions on Vehicular Technology, vol. vt-33, no.4, November 1984.

[Smith94] Smith, W.S., and P. H. Wittke, "Differential Detection of GMSK in Rician Fading", IEEE Transactions on Communications, vol. 42, no. 2/3/4, February/March/April, 1994.

[Stew95] Steward, Shawn, "Packet or Circuit: Deciding Factors", Cellular Business, p. 18, July 1995.

[Taylor95] Taylor, R., S. Arnold, and M. Wallace, "A CDPD Performance Model for an Intelligent Transportation System Architecture Evaluation, Proceedings of Virginia Tech's Fifth Symposium On Wireless Personal Communications, May31 - June 2, 1995.

[Var91] Varshney, P. and S. Kumar, "Performance of GMSK in a Land Mobile Radio Channel", IEEE Transactions on Vehicular Technology, vol. 40, no. 3, August 1991.

[Var93] Varshney, P., J. E. Salt and S. Kumar, "BER Analysis of GMSK with Differential Detection in a Land Mobile Channel", IEEE Transactions on Vehicular Technology, vol. 42, no. 4, November 1993.

[Var94] -----, "Performance of GMSK with Two-Bit Differential Detection in a Land Mobile Radio Channel", Can. J. Elect. & Comp. Eng., vol 19, no. 1, 1994.

[Yong88] Yongacoglu, A., D. Makrakis, K. Feher, "Differential Detection of GMSK Using Decision Feedback", IEEE Transactions On Communications, vol 36, no. 6, June 1988.

Appendix A - Execution Instructions

The simulation models for the CDPD channels can be found in the directory

/home/u6/csi3.1/caedata/elsonlib2

Any custom-coded blocks that were created in the development of the communications system are predominantly found in the directory

/home/u6/csi3.1/caedata/elsonlib

with the exception of one or two which may be in the previous directory. The SPW filenames are named according to the simulation and follow the format

chan_sim_rec

where ***chan*** is the channel on which the simulation was performed, forward or reverse, denoted by a ***r*** or a ***f***. ***sim*** is the actual simulation that was performed such as ***awgn*** for Gaussian noise, or ***fade8*** for Rayleigh fading with a vehicle speed of 8 km/hr. ***rec*** denotes the receiver type, either ***fd*** for frequency discriminator or ***dd*** for differential detection. Therefore a typical file name would be

r_fade50_dd

denoting a Rayleigh fading simulation on the reverse channel using differential detection.

Assuming some knowledge of SPW, the selected file would be opened in SPW's Block Diagram Editor and the simulation parameters can be set, i.e. noise power, Doppler frequency. To execute the simulation, choose **Tools | Simulator | Run** form the BDE menus. This will bring up a simulator window with the current filename. Make sure the correct pool is selected for the simulation, this will be one of two named

el_rchan_pool or ***el_fchan_pool***

These pools list all the blocks used in the simulations for each channel, including custom-coded blocks.

Under the Run To option choose EOF for End Of File. The simulations are set up so that they will run until the end of the file is reached or 15 block errors are encountered.

Three different length files were used during simulations depending on the signal strength and the amount of time it took to reach 15 block errors. They are found in the directory

/home/u6/csi3.1/spwdata/elsonsigs

and are named

rand_data.sig - file with data for the simulation of 100,000 RS blocks

rand_data2.sig - file with data for the simulation of 10,000 RS blocks

rand_data3.sig - file with data for the simulation of 1000 RS blocks

Three more files of random data of the same length were created for use in co-channel interference simulations. These are name din the same way except for the *rand2* label. Shorter length files were used at lower SNR's to save time when data is being loaded into SPW's Signal Calculator. Longer data files were needed at high SNR's in order to obtain 15 block errors. Attempts to create data files larger than *rand_data.sig* resulted in errors involving not enough memory for their creation.

Once the simulation has completed, results can be viewed in the Signal Calculator by pressing the Sig Calc button in the Simulator window. A number of data files will appear in the Signal Calculator and the following file names yield

und_bit.sig	- the total number of bit errors
und_blk.sig	- the total number of block errors
bit7.sig	- number of bit errors correcting 7 symbol errors
blk7.sig	- number of block errors correcting 7 symbol errors
sym_blk.sig	- the number of symbol errors per block

sym_tot.sig - the total number of symbol errors
r_dot_err.sig - bit errors in the reverse channel dotting sequence
r_synch_err.sig- bit errors in the reverse channel synchronization word

The Signal Calculator will also show the input data file that was used for the simulation.

VITA

James Scott Elson was born in Rockhill, South Carolina on July 21st, 1971. He completed his B.S. in Electrical Engineering in May 1993 at Virginia Polytechnic Institute and State University and went on to pursue his Master's in the same field which has resulted in this work. While completing his studies in Blacksburg, he was a four-year letterman for the Virginia Tech Men's Soccer program and a member of the Sigma Chi Fraternity. Scott is currently working for the Grayson Electronics Research and Development Office in Blacksburg, Virginia, the sponsor of this research.